



PLASMA: Parallel Linear Algebra Software for Multicore Using OpenMP

Journal:	<i>Transactions on Mathematical Software</i>
Manuscript ID	TOMS-2017-0061.R1
Manuscript Type:	5 Regular Paper for RCR Initiative
Date Submitted by the Author:	n/a
Complete List of Authors:	<p>Dongarra, Jack; University of Tennessee, Department of Electrical Engineering & Computer Science Gates, Mark; University of Tennessee, Department of Electrical Engineering & Computer Science Haidar, Azzam; University of Tennessee, Department of Electrical Engineering & Computer Science Kurzak, Jakub; University of Tennessee, Department of Electrical Engineering & Computer Science Luszczek, Piotr; University of Tennessee, Department of Electrical Engineering & Computer Science Wu, Panruo; University of Tennessee, Department of Electrical Engineering & Computer Science Yamazaki, Ichitaro; University of Tennessee, Department of Electrical Engineering & Computer Science YarKhan, Asim; University of Tennessee, Department of Electrical Engineering & Computer Science Abalenkovs, Maksims; The University of Manchester, School of Mathematics Bagherpour, Negin; The University of Manchester, School of Mathematics Hammarling, Sven; The University of Manchester, School of Mathematics Sistik, Jakub; The University of Manchester, School of Mathematics</p>
Computing Classification Systems:	Mathematics of computing~Mathematical software performance, Mathematics of computing~Solvers, Computing methodologies~Shared memory algorithms



PLASMA: Parallel Linear Algebra Software for Multicore Using OpenMP

JACK DONGARRA, MARK GATES, AZZAM HAIDAR, JAKUB KURZAK, PIOTR LUSZCZEK, PANRUO WU, ICHITARO YAMAZAKI, and ASIM YARKHAN, University of Tennessee, USA
 MAKSIMS ABALENKOV, NEGIN BAGHERPOUR, SVEN HAMMARLING, JAKUB ŠÍSTEK, DAVID STEVENS, and MAWUSSI ZOUNON, The University of Manchester, UK
 SAMUEL D. RELTON, The University of Leeds, UK

The recent version of the PLASMA (Parallel Linear Algebra Software for Multicore Architectures) library is based on tasks with dependencies from the OpenMP standard. The main functionality of the library is presented. Extensive benchmarks are targeted on three recent multicore and manycore architectures, namely an Intel Xeon, Intel Xeon Phi, and IBM POWER 8 processors.

CCS Concepts: • **Mathematics of computing** → **Mathematical software performance**; *Solvers*; • **Computing methodologies** → *Shared memory algorithms*;

Additional Key Words and Phrases: Numerical linear algebra libraries, tile algorithms, task-based programming, multicore processors, OpenMP, PLASMA

ACM Reference Format:

Jack Dongarra, Mark Gates, Azzam Haidar, Jakub Kurzak, Piotr Luszczek, Panruo Wu, Ichitaro Yamazaki, Asim YarKhan, Maksims Abalenkovs, Negin Bagherpour, Sven Hammarling, Jakub Šístek, David Stevens, Mawussi Zounon, and Samuel D. Relton. 2017. PLASMA: Parallel Linear Algebra Software for Multicore Using OpenMP. *ACM Trans. Math. Softw.* 0, 0, Article 00 (2017), 35 pages. <https://doi.org/0000001.0000001>

1 INTRODUCTION

The PLASMA numerical library (*Parallel Linear Algebra Software for Multicore Architectures*) is a dense linear algebra package at the forefront of multicore computing. PLASMA has been a response to the advent of multicore processors, proclaimed in the prominent 2005 article by Herb Sutter, “The Free Lunch Is Over: A Fundamental Turn Toward Concurrency in Software” in Dr. Dobb’s Journal [Sutter 2005]. At that time, it became apparent that both LAPACK¹ [Anderson

¹<http://www.netlib.org/lapack>

The authors thank the Intel Corporation for their generous hardware donation and continuous financial support. They also thank the Oak Ridge Leadership Computing Facility for providing access to the POWER8 system. This work has been supported by the National Science Foundation under grants CCF-1339822 (SILAS) and CCF-1527706 (DARE), by the European Commission H2020 projects 671633 (NLAFET) and 671602 (INTERTWinE), and by the Engineering and Physical Sciences Research Council project EP/M01147X/1 (SERT).

Authors’ addresses: Jack Dongarra; Mark Gates; Azzam Haidar; Jakub Kurzak; Piotr Luszczek; Panruo Wu; Ichitaro Yamazaki; Asim YarKhan, University of Tennessee, Department of Electrical Engineering & Computer Science, Knoxville, TN, 37996-3450, USA; Maksims Abalenkovs; Negin Bagherpour; Sven Hammarling; Jakub Šístek; David Stevens; Mawussi Zounon, The University of Manchester, School of Mathematics, Manchester, M13 9PL, UK; Samuel D. Relton, The University of Leeds, Institute of Health Sciences, Leeds, LS2 9LJ, UK.

Permission to make digital or hard copies of all or part of this work for personal or classroom use is granted without fee provided that copies are not made or distributed for profit or commercial advantage and that copies bear this notice and the full citation on the first page. Copyrights for components of this work owned by others than ACM must be honored. Abstracting with credit is permitted. To copy otherwise, or republish, to post on servers or to redistribute to lists, requires prior specific permission and/or a fee. Request permissions from permissions@acm.org.

© 2017 Association for Computing Machinery.

Manuscript submitted to ACM

Manuscript submitted to ACM

53 et al. 1999] and ScaLAPACK² [Blackford et al. 1997] were ill suited for efficient multicore execution. Initial work focused
54 on efficient multithreading of standard dense linear algebra algorithms (LU with partial pivoting, Cholesky, QR) using
55 the canonical, column-major, data layout of LAPACK [Kurzak and Dongarra 2006]. The debut of the STI Cell processor
56 in 2006 pushed the developments in new directions.
57

58 The most influential aspect of the STI Cell was the memory architecture based on software controlled caches. This
59 motivated tiling of the input matrices for efficient communication between the main memory and the caches. The
60 memory architecture, and its high internal bandwidth, promoted systolic algorithms with high degrees of pipelining.
61 At the same time, the 14× performance advantage of single precision over double precision, in the original Cell design,
62 stimulated the development of mixed precision algorithms. Notable papers from that era highlighted tiling, scheduling,
63 and mixed precision iterative refinement [Buttari et al. 2007; Gustavson et al. 2012; Kurzak et al. 2008; Kurzak and
64 Dongarra 2007, 2009; Langou et al. 2006]. All these artifacts influenced the design of the PLASMA library in one form
65 or another.
66

67
68 Seminal to PLASMA developments was also the idea of superscalar scheduling, which also gained initial traction as
69 a solution for the Cell processor [Bellens et al. 2006]. The CellSs system from the Barcelona Supercomputer Center
70 served as the initial inspiration for the development of the QUARK scheduler and its subsequent adoption in PLASMA
71 alongside Pthreads-based routines [Kurzak et al. 2013].
72

73 Before PLASMA managed to get significant traction with the user community, GPUs entered the mainstream of
74 HPC, and the MAGMA library [Agullo et al. 2009] became the focal point of dense linear algebra developments at UTK.
75 Due to the differences between GPUs and multicore processors, the design of MAGMA differs significantly from that
76 of PLASMA. Nevertheless, throughout its existence, PLASMA has served as a tremendous research vehicle for the
77 development of new algorithms and scheduling techniques.
78

79 Eventually, adoption of superscalar scheduling in the OpenMP standard motivated the retirement of QUARK in
80 favor of OpenMP, as well as retirement of the Pthreads routines. This transition was decided after our successful first
81 experiments with selected functions using the OpenMP tasks summarized in [YarKhan et al. 2016].
82

83 This article describes the final design of the OpenMP version of PLASMA, and assesses performance on a variety of
84 current multicore hardware configurations for a large set of routines. The most recent version, PLASMA 17³, offers an
85 extensive collection of optimized routines for solving linear systems of equations and least squares problems.
86

87 PLASMA is designed to deliver high performance from a system with multiple sockets of multicore processors, an
88 objective achieved by combining state of the art solutions in parallel algorithms, scheduling, and software engineering.
89 In particular, PLASMA is built around the following three concepts.
90

91 *Tile Matrix Layout.* PLASMA utilizes a tile-based storage approach. The matrix is subdivided into square blocks,
92 called *tiles*, of relatively small size, with each tile occupying a continuous memory region. Tiles are loaded to the cache
93 memory efficiently with little risk of eviction while being processed. The use of the tile layout minimizes conflict
94 cache misses, translation lookaside buffer (TLB) misses, and false sharing, and maximizes potential for prefetching.
95 PLASMA contains parallel and cache efficient routines for converting between the conventional column-major and
96 the tile layouts. PLASMA currently stores both versions of the matrices, so it has larger memory requirements than
97 LAPACK.
98
99

100
101
102 ²<http://www.netlib.org/scalapack>

103 ³<https://bitbucket.org/icl/plasma>

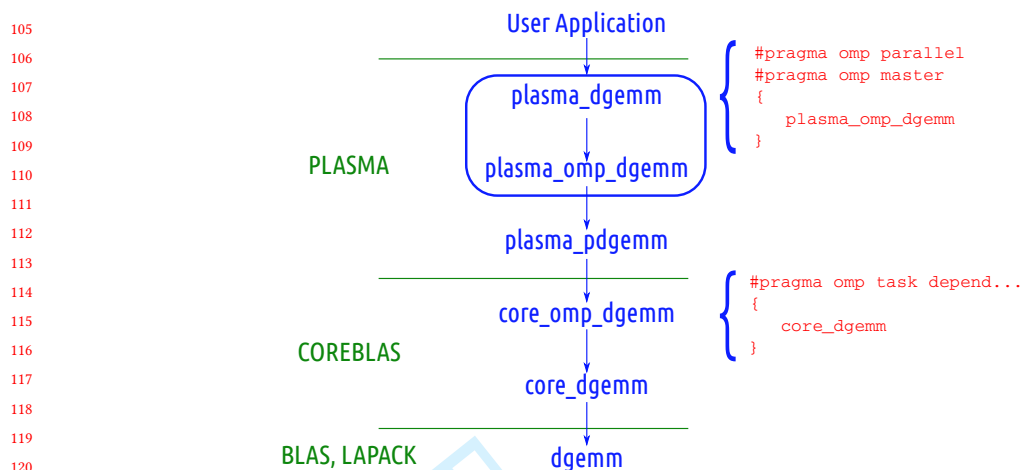


Fig. 1. Overview of PLASMA structure with key parts of the OpenMP implementation. User-level routines are in the box.

Tile Algorithms. PLASMA is based on algorithms redesigned to work on tiles, which maximize data reuse in the cache levels of multicore systems. Tiles are loaded to the cache and processed completely before being transferred back to the main memory. Operations on small tiles create fine grained parallelism providing enough work to keep a large number of cores occupied. Initial work on tile algorithms was published in [Agullo et al. 2009; Buttari et al. 2009], and a recent overview for the development of tile algorithms can be found in [Abdelfattah et al. 2016].

Dynamic Scheduling. PLASMA relies on concurrent runtime scheduling of sequential tasks. Runtime scheduling is based on the idea of assigning work to cores based on the availability of data for processing at any given point in time, and thus is also sometimes called data-driven scheduling. The concept is related closely to the idea of expressing computation through a task graph, often referred to as the DAG (Directed Acyclic Graph), and the flexibility of exploring the DAG at runtime. This is in direct opposition to the fork-and-join scheduling, where artificial synchronization points expose serial sections of the code and multiple cores are idle while sequential processing takes place. Currently, PLASMA relies on OpenMP for dynamic, task-based, scheduling. Comparison of the two runtimes for PLASMA was presented in [YarKhan et al. 2016] showing that the more general-purpose tasks of OpenMP are able to provide the same performance as the more specialized QUARK. PLASMA makes use of tasks with dependencies and priorities, therefore a compiler supporting these features of the OpenMP 4.5 standard is required.

The asynchronous execution of the sequential tasks generally makes very efficient use of the hardware, leading to compact traces throughout the majority of the runtime. Traces typically become sparse only at the very beginning or end of the algorithm, where algorithms do not expose enough parallelism and communication costs may dominate.

2 ALGORITHMS IN PLASMA

2.1 Structure of PLASMA

PLASMA closely follows the structuring of functionality found in the LAPACK and BLAS libraries [Dongarra et al. 1990a,b, 1988a,b; Lawson et al. 1979]. Let us take the example of matrix-matrix multiply in double real precision; the

	real	complex
64 bit (double)	d gemm	z gemm
32 bit (single)	s gemm	c gemm

Table 1. An example of the naming conventions for matrix matrix multiply (\square gemm).

well known dgemm routine. Four different versions are provided for most subroutines, related to different data precisions and distinguished by the leading letter; see Table 1. We use \square as a generic symbol for any of these precisions.

The PLASMA routine stack is depicted in Fig. 1. Two different levels of functions are exposed to the user. The top level function, `plasma_dgemm`, is a parallel analog of the dgemm from BLAS; see the listing in Fig. 2. Note that this is rather different from the implementation in the well known PBLAS library⁴ for distributed memory architectures. During the execution of this function, a parallel section of OpenMP is opened by `#pragma omp parallel`. This is where a number of OpenMP threads are spawned, as specified by the `OMP_NUM_THREADS` environment variable. All of the code within this block is executed by the master thread only; note the `#pragma omp master` directive in Fig. 2. Tasks are generated by the master thread, inside the function calls within the parallel region, and are executed by all the available threads in an asynchronous manner. The master thread proceeds to the end of the parallel region, where it joins the working threads in executing the tasks it has produced. The end of the parallel block acts as a synchronization point, and the execution proceeds beyond this point only after all the tasks have been completed and OpenMP threads closed.

The second level functions in this example are `plasma_omp_zge2desc`, `plasma_omp_dgemm`, and `plasma_omp_zdesc2ge`. The `plasma_omp_zge2desc` and `plasma_omp_zdesc2ge` functions serve for translation of the data layout between LAPACK column-major and tile storage; see Section 2.8. The main function here is `plasma_omp_dgemm`, which is also exposed to the user, and its simplified body is shown in Fig. 3. For our chosen dgemm example this function contains just one call to an internal routine with a tile algorithm; i.e. `plasma_pdgemm`, however multiple algorithms may be combined on this level. Combining multiple algorithms in this way allows their execution to overlap in an asynchronous manner. This overlap of algorithms can significantly reduce the overall execution time for these combined functions, and it is one of the main strengths of PLASMA. This is also the primary reason for exposing the second level of PLASMA functions, which an advanced user can fuse in a custom order inside a user-defined OpenMP parallel region. **This interface also allows an advanced user to have fine control over the number of OpenMP threads and their placement. For example, one can run a PLASMA algorithm on a prescribed number of threads specified at the `#pragma omp parallel` clause by the `num_threads()` keyword.**

The heart of PLASMA, a tile-based algorithm, is implemented inside the `plasma_pdgemm` function; see Fig. 4. Inside this function, which is still executed only by the master thread, loops over matrix tiles appear and functions that process tiles are called. These functions, also called *computational kernels*, are part of the COREBLAS library, which forms a self-standing part of PLASMA.

In the dgemm example, the only computational kernel involved is the `core_omp_dgemm` function, see Fig 5. An OpenMP task with data dependencies is generated inside this function by the master thread and enqueued into the OpenMP runtime. From the body of the task, a call to the `core_dgemm` function (Fig. 6) is made. In this example the task consists of calling a sequential version of the dgemm routine from the CBLAS library (i.e. a C wrapper of BLAS), involving three tiles. In general, the sequential kernels in PLASMA map to simple calls to BLAS routines, calls to LAPACK routines, or custom implementations derived specifically for tile algorithms (e.g. in the case of the QR factorization). The reason for

⁴http://www.netlib.org/scalapack/pblas_qref.html

```

209 int plasma_dgemm(plasma_enum_t transA, plasma_enum_t transB,
210                 double alpha, double *pA, int lda,
211                 double *pB, int ldb,
212                 double beta, double *pC, int ldc)
213 {
214     ...
215     // asynchronous block
216     #pragma omp parallel
217     #pragma omp master
218     {
219         // Translate matrices from LAPACK to tile layout
220         plasma_omp_zge2desc(pA, lda, A);
221         plasma_omp_zge2desc(pB, ldb, B);
222         plasma_omp_zge2desc(pC, ldc, C);
223
224         // Call the asynchronous function
225         plasma_omp_dgemm(transA, transB,
226                         alpha, A,
227                         B,
228                         beta, C);
229
230         // Translate result back to LAPACK layout
231         plasma_omp_zdesc2ge(C, pC, ldc);
232     }
233     // implicit synchronization
234     ...
235 }

```

Fig. 2. An example of the `plasma_dgemm` top-level function. Only the master thread executes the code in the parallel block, then creates and enqueues sequential tasks. The `plasma_omp_zge2desc` and `plasma_omp_zdesc2ge` serve for translating a matrix from LAPACK to tile layout of the PLASMA matrix descriptor and vice versa.

```

239 void plasma_omp_dgemm(plasma_enum_t transA, plasma_enum_t transB,
240                     double alpha, plasma_desc_t A,
241                     plasma_desc_t B,
242                     double beta, plasma_desc_t C)
243 {
244     // Call the parallel function
245     plasma_pdgemm(transA, transB,
246                 alpha, A,
247                 B,
248                 beta, C);
249 }

```

Fig. 3. An example of the second-level function `plasma_omp_dgemm`. The code is executed only by the master thread.

separating the `core_omp_dgemm` function, which creates the task, from the `core_dgemm`, which implements the kernel is allowing the same kernel to be used from different runtime systems, and even from outside of PLASMA (e.g. by the DPLASMA library [Bosilca et al. 2011, 2010a,b, 2012]⁵).

⁵<http://icl.cs.utk.edu/dplasma>

6

Dongarra, J. et al

```

261 #define A(m, n) (double*)plasma_tile_addr(A, m, n)
262 #define B(m, n) (double*)plasma_tile_addr(B, m, n)
263 #define C(m, n) (double*)plasma_tile_addr(C, m, n)
264
265 void plasma_pdgemm(plasma_enum_t transA, plasma_enum_t transB,
266                  double alpha, plasma_desc_t A, plasma_desc_t B,
267                  double beta, plasma_desc_t C)
268 {
269     for (int m = 0; m < C.mt; m++) {
270         int mvcm = plasma_tile_mview(C, m);
271         int ldcm = plasma_tile_mmain(C, m);
272         for (int n = 0; n < C.nt; n++) {
273             int nvcn = plasma_tile_nview(C, n);
274             if (transA == PlasmaNoTrans && transB == PlasmaNoTrans) {
275                 for (int k = 0; k < A.nt; k++) {
276                     int nvak = plasma_tile_nview(A, k);
277                     int ldbk = plasma_tile_mmain(B, k);
278                     double zbeta = k == 0 ? beta : 1.0;
279
280                     // Call the kernel
281                     core_omp_dgemm(transA, transB,
282                                 mvcm, nvcn, nvak,
283                                 alpha, A(m, k), ldcm,
284                                 B(k, n), ldbk,
285                                 zbeta, C(m, n), ldcm);
286                 }
287             }
288         }
289     }
290 }

```

Fig. 4. Skeleton of the tile matrix multiply `plasma_pdgemm`. The `mt` and `nt` are numbers of rows and columns of tiles of a matrix stored in the tile layout. The macros `A(m, n)`, `B(m, n)`, and `C(m, n)` at the top expand to the `plasma_tile_addr` function, which returns the address of the first entry of the tile on the m -th tile-row and in the n -th tile-column of the corresponding matrix. The `plasma_tile_mview` and `plasma_tile_nview` functions return the number of rows and columns in a local tile. The `plasma_tile_mmain` function returns the leading dimension of the tile, which can be different from m if the matrix descriptor is a submatrix (called 'view') of another matrix descriptor without a deep data copy.

2.2 Parallel BLAS

PLASMA contains a full set of routines from the Level 3 BLAS; see Table 2. BLAS routines in PLASMA are parallelized by tiling. Their implementations are mostly straightforward loop nests, and individual tasks are essentially calls to sequential BLAS. The listing in Fig. 4 has already shown the simplified tile matrix matrix multiplication (`plasma_pdgemm` routine).

Parallel BLAS routines in PLASMA are algorithmically equivalent to their reference Netlib implementations⁶.

2.3 Parallel Norms

PLASMA contains a set of routines for computing matrix norms, specifically the *max*, *one*, *infinity*, and *Frobenius* norms. PLASMA employs tiling for increased parallelism within the norm computations. While being mostly memory bound, PLASMA norm routines still benefit from multithreading, as usually a single core cannot saturate the memory

⁶<http://www.netlib.org/blas>

```

313 void core_omp_dgemm(plasma_enum_t transA, plasma_enum_t transB,
314                   int m, int n, int k,
315                   double alpha, const double *A, int lda,
316                   const double *B, int ldb,
317                   double beta, double *C, int ldc)
318 {
319     int ak = (transA == PlasmaNoTrans) ? k : m;
320     int bk = (transB == PlasmaNoTrans) ? n : k;
321     #pragma omp task depend(in:A[0:lda*ak]) \
322     depend(in:B[0:ldb*bk]) \
323     depend(inout:C[0:ldc*n])
324     {
325         core_dgemm(transA, transB,
326                 m, n, k,
327                 alpha, A, lda,
328                 B, ldb,
329                 beta, C, ldc);
330     }
331 }

```

Fig. 5. An example of the definition of the sequential `core_omp_dgemm` task. The OpenMP task consists of a call to sequential `core_dgemm` routine. Some parameters have been omitted for brevity.

```

333 void core_dgemm(plasma_enum_t transA, plasma_enum_t transB,
334               int m, int n, int k,
335               double alpha, const double *A, int lda,
336               const double *B, int ldb,
337               double beta, double *C, int ldc)
338 {
339     cblas_dgemm(CblasColMajor,
340               transA, transB,
341               m, n, k,
342               alpha, A, lda,
343               B, ldb,
344               beta, C, ldc);
345 }

```

Fig. 6. An example of the definition of the sequential `core_dgemm` kernel. In this example, the function just calls a sequential BLAS `dgemm` routine. Some parameters have been omitted for brevity.

Table 2. Level 3 BLAS routines.

Name	Description
<code>sgemm</code>	matrix matrix multiply
<code>shemm</code>	Hermitian matrix matrix multiply
<code>sher2k</code>	Hermitian rank-2k update to a matrix
<code>sherk</code>	Hermitian rank-k update to a matrix
<code>ssymm</code>	symmetric matrix matrix multiply
<code>ssyr2k</code>	symmetric rank-2k update to a matrix
<code>ssyrk</code>	symmetric rank-k update to a matrix
<code>strmm</code>	triangular matrix matrix multiply
<code>strsm</code>	triangular solve with multiple right hand sides

Name	Description
<code>dlange</code>	norm of a (general) matrix
<code>dlanhe</code>	norm of a Hermitian matrix
<code>dlansy</code>	norm of a symmetric matrix
<code>dlantr</code>	norm of a triangular or trapezoidal matrix

Table 3. Matrix norm routines.

Name	Description	Definition
<code>PlasmaMaxNorm</code>	max norm - maximum absolute value	$\ A\ _{\max} = \max_{1 \leq i \leq m, 1 \leq j \leq n} a_{ij} $
<code>PlasmaOneNorm</code>	one norm - maximum column sum	$\ A\ _1 = \max_{1 \leq j \leq n} \sum_{i=1}^m a_{ij} $
<code>PlasmaInfNorm</code>	infinity norm - maximum row sum	$\ A\ _{\infty} = \max_{1 \leq i \leq m} \sum_{j=1}^n a_{ij} $
<code>PlasmaFrobeniusNorm</code>	Frobenius norm - square root of sum of squares	$\ A\ _F = \left(\sum_{i=1}^m \sum_{j=1}^n a_{ij} ^2 \right)^{1/2}$

Table 4. Matrix norm types.

bandwidth. Table 3 lists all the norm routines implemented in PLASMA, and Table 4 lists all the types of norms supported.

An example of the tile version of the function computing the *one* norm of a general matrix is provided in Fig. 7. In this routine, the vector of column sums is first computed for each tile. Then the partial results are combined in a final reduction step. In the *infinity* norm routine, the same approach is applied row-wise. In the *Frobenius* norm routine, the sum of squares is computed for each tile, then the partial results are combined, and then the square root is taken. The *Frobenius* norm follows the LAPACK approach of scaling the results along the way, to minimize roundoff errors (See the LAPACK `lassq` routine for details). In general, computing partial sums should be beneficial, rather than detrimental, to the numerical stability of the norm computations. Tiling has no effect on the *max* norm, as the operation is order invariant.

In Fig. 7, the `core_omp_dlange` kernel is just a simple call to the sequential `dlange` function from LAPACK, which computes the matrix norm of the tile. The `core_omp_dlange_aux` kernel is a custom kernel computing the row or column sums of the tile into a vector without finding their maxima.

In addition, PLASMA contains the `[dz]sc[d]samax` routine, which computes the *max* norm for each column of a matrix, and returns the result as a vector. This routine is needed for checking the convergence of the solution in the iterative refinement process of the mixed precision solvers; see Section 2.5.

2.4 Linear Systems

PLASMA contains a set of routines for solving linear systems of equations, both full and band. Routines for solving general systems of equations rely on the LU factorization with partial (row) pivoting, routines for solving symmetric positive definite (SPD) systems rely on the Cholesky factorization, and routines for solving symmetric (not necessarily positive definite) systems rely on the LDL^T factorization by Aasen's algorithm [Aasen 1971].

```

417 void plasma_pdlange(plasma_enum_t norm,
418                   plasma_desc_t A, double *work, double *value)
419 {
420     switch (norm) {
421         double *workspace;
422
423     case PlasmaOneNorm:
424         for (int m = 0; m < A.mt; m++) {
425             int mvam = plasma_tile_mview(A, m);
426             int ldam = plasma_tile_mmain(A, m);
427
428             for (int n = 0; n < A.nt; n++) {
429                 int nvan = plasma_tile_nview(A, n);
430
431                 core_omp_dlange_aux(PlasmaOneNorm,
432                                   mvam, nvan,
433                                   A(m, n), ldam,
434                                   &work[A.n*m+n*A.nb]);
435             }
436         }
437         #pragma omp taskwait
438         workspace = work + A.mt*A.n;
439         core_omp_dlange(PlasmaInfNorm,
440                       A.n, A.mt,
441                       work, A.n,
442                       workspace, value);
443     case ...
444         // Other options were omitted from the listing.
445     }
446 }
447
448
449
450
451
452
453
454
455
456
457
458
459
460
461
462
463
464
465
466
467
468

```

Fig. 7. Example of the routine for norm of a general matrix `plasma_pdlange`. Only the *one*-norm branch is kept in the listing. The `#pragma omp taskwait` is a necessary synchronization and the master thread waits for completion of all the enqueued tasks before proceeding to the final accumulation. The `work` and `workspace` arrays contain memory preallocated by the user that is used by the subroutines for intermediate storage. The listing has been simplified for brevity.

Dense. Table 5 lists all the linear systems routines implemented in PLASMA. Like LAPACK, PLASMA provides a routine for solving a system of linear equations, as well as a routine for only factoring the matrix, and a routine for solving a system using a previously factored matrix. This allows for a matrix to be factorized once, and reusing the result for repeatedly solving different right hand sides.

Band. Table 6 lists all the band linear solvers that PLASMA implements. PLASMA's nonsymmetric band linear solver is based on a band version of the LU factorization, while for solving an SPD band system of linear equations, it uses a band version of the Cholesky factorization.

To maintain the numerical stability, our band LU routine performs partial (row) pivoting. When the pivoting is applied to the previous columns of L , it could completely destroy its band structure. In order to avoid these fills, LAPACK only applies the pivoting to the remaining columns. On the other hand, PLASMA's band LU routine relies on the PLASMA's LU panel factorization routine that explicitly applies the pivots to the previous columns within the panel. Hence, though PLASMA returns the LU factors in the LAPACK's band matrix format, to store these potential fills, its leading dimension must accommodate the additional $n_d - 1$ entries on the bottom, where n_d is the tile size.

Name	Description
<code>□gesv</code>	linear system solve
<code>□getrf</code>	triangular factorization
<code>□getrs</code>	linear system solve (previously factored)
<code>[z c] hesv</code>	Hermitian linear system solve
<code>[z c] hetrf</code>	Hermitian triangular factorization
<code>[z c] hetrs</code>	Hermitian linear system solve (previously factored)
<code>□posv</code>	positive definite linear system solve
<code>□potrf</code>	positive definite triangular factorization
<code>□potrs</code>	positive definite linear system solve (previously factored)
<code>[d s] sysv</code>	symmetric linear system solve
<code>[d s] sytrf</code>	symmetric triangular factorization
<code>[d s] sytrs</code>	symmetric linear system solve (previously factored)

Table 5. Linear systems routines.

Name	Description
<code>□gbsv</code>	band linear system solve
<code>□gbtrf</code>	band triangular factorization
<code>□gbtrs</code>	band linear system solve (previously factored)
<code>□pbsv</code>	band positive definite linear system solve
<code>□pbtrf</code>	band positive definite triangular factorization
<code>□pbtrs</code>	band positive definite linear system solve (previously factored)

Table 6. Band linear systems routines.

Algorithm 1: Cholesky-based solution of $AX = B$ (`plasma_omp_dposv`)

Data: A, B

Result: X

$A = LL^T$ Cholesky factorization of matrix A , `plasma_pdpotrf`;

$LY = B$ forward solve, `plasma_pdtrsm`;

$L^T X = Y$ backward solve, `plasma_pdtrsm`;

2.4.1 Cholesky factorization. The Cholesky factorization is a straightforward algorithm to be written in the tile-oriented fashion [Buttari et al. 2009; Haidar et al. 2011], and Fig. 8 shows the algorithm used in PLASMA. Apart from using the `core_omp_dgemm` kernel from Fig. 5, it uses the `core_omp_dpotrf` kernel for Cholesky factorization of a tile by calling the LAPACK `dpotrf` function, the `core_omp_dtrsm` function for solving a system with a triangular matrix, and the `core_omp_dsyrc` for a rank- k update of a symmetric matrix.

The Cholesky factorization is the basis for solving linear systems of equations, where coefficients form a symmetric positive definite (SPD) matrix. It is part of the `plasma_omp_□posv` routine (Algorithm 1), in which the individual stages are overlapped. A call to the `plasma_□potrf` routine should also precede a call to the `plasma_□potrs` routine, which can be called repeatedly for new right hand sides, and uses the Cholesky factors as input. While this version based on the top-level PLASMA interfaces would not be overlapped, doing the same with the second-level interfaces of `plasma_omp_□potrf` and `plasma_omp_□potrs` allows a user to benefit from the overlapping. Cholesky factorization is also the basis for computing the inverse of an SPD matrix, see Section 2.6.

```

521 void plasma_pdpotrf(plasma_enum_t uplo, plasma_desc_t A)
522 {
523     if (uplo == PlasmaUpper) {
524         for (int k = 0; k < A.nt; k++) {
525             int nvak = plasma_tile_nview(A, k);
526             int ldak = plasma_tile_mmain(A, k);
527
528             core_omp_dpotrf(PlasmaUpper, nvak,
529                             A(k, k), ldak);
530
531             for (int m = k+1; m < A.nt; m++) {
532                 int nvam = plasma_tile_nview(A, m);
533                 core_omp_dtrsm(PlasmaLeft, PlasmaUpper,
534                               PlasmaConjTrans, PlasmaNonUnit,
535                               A.nb, nvam,
536                               1.0, A(k, k), ldak,
537                               A(k, m), ldak);
538             }
539             for (int m = k+1; m < A.nt; m++) {
540                 core_omp_dsyrk(
541                     PlasmaUpper, PlasmaConjTrans,
542                     nvam, A.mb,
543                     -1.0, A(k, m), ldak,
544                     1.0, A(m, m), ldam);
545
546                 for (int n = k+1; n < m; n++) {
547                     core_omp_dgemm(
548                         PlasmaConjTrans, PlasmaNoTrans,
549                         A.mb, nvam, A.mb,
550                         -1.0, A(k, n), ldak,
551                         A(k, m), ldak,
552                         1.0, A(n, m), ldan);
553                 }
554             }
555         }
556     }
557     else {
558         // This option was omitted from the listing.
559     }
560 }

```

Fig. 8. Algorithm for the Cholesky factorization `plasma_pdpotrf`. Only the branch for storing the upper triangle of the matrix is shown. The listing has been simplified for brevity.

2.4.2 LU factorization. The critical component of the LU factorization is the step of factoring a panel, which in PLASMA is a column of tiles. This operation is on the critical path of the algorithm and has to be optimized to the fullest. At the same time, a naive implementation, such as the `qgetf2` routine in LAPACK, is memory bound.

The current implementation of the LU panel factorization in PLASMA is a result of convergence of multiple different research efforts, specifically the work on *Parallel Cache Assignment (PCA)* by Castaldo et al. [Castaldo and Whaley 2010], and the work on parallel recursive panel factorization by Dongarra et al. [Dongarra et al. 2014]. Also, the survey by Donfack et al. [Donfack et al. 2015] provides a good overview of different implementations of the LU factorization.

The panel factorization is shown in Fig. 9. It relies on internal blocking and persistent assignment of tiles to threads. Unlike past implementations, it is not recursive, as plain recursion proved inferior to blocking. Memory residency provides cache reuse for the factorization of sub-panels, while blocking provides some level of compute intensity for

Algorithm 2: LU-based solution of $AX = B$ (plasma_omp_dgesv)**Data:** A, B **Result:** X $PA = LU$ LU factorization of matrix A , plasma_pdgetrf; $\tilde{B} = PB$ row permutation of B , plasma_pdgeswp; $LY = \tilde{B}$ forward solve, plasma_pdtrsm; $UX = Y$ backward solve, plasma_pdtrsm;

the sub-tile update operations. The result is an implementation that is not memory bound and scales well with the number of cores.

Priorities on tasks serve as hint for the OpenMP runtime to schedule the tasks on the critical path, namely the panel factorization, the update of the subsequent block column, and their nested tasks, as soon as their dependencies are satisfied.

The complete LU factorization, including the panel factorization, and the updates to the trailing submatrix, is multithreaded differently than other operations in PLASMA. Due to some operations affecting entire columns of tiles, data-dependent tasks are created for column operations, not tile operations, i.e., dependency tracking is resolved at the granularity of columns, not individual tiles. To allow transition between the tile-oriented algorithms and the column-oriented LU, dummy tasks have been introduced. These tasks do not perform any useful work, and their only purpose is inserting data dependencies of the column on all its tiles and vice versa. This translation of data dependency seems needed due to the lack of multi-dependencies in OpenMP, which would allow a loop over addresses in the depend clause. An example of dummy tasks inserted in front of the panel factorization is shown in Fig. 10.

Nested tasks are created within each panel factorization, and internally synchronized using thread barriers. Similarly, nested tasks are created within each column of \square gemm updates, and synchronized with the `#pragma omp taskwait` clause, before exiting the parent task. Waiting for completion of the nested tasks is necessary for correct dependency-tracking at the column granularity.

The LU factorization is the basis for routines for solving systems of linear equations. It is part of the `plasma_omp_□gesv` routine (Algorithm 2), in which the individual stages are overlapped. A call to the `plasma_dgetrf` routine should also precede a call to the `plasma_dgetrs` routine, which can be called repeatedly for new right hand sides, and uses the LU factors as input.

2.4.3 LDL^T factorization. To solve a symmetric indefinite linear system, PLASMA first reduces the symmetric matrix into a band form by the tiled Aasen's algorithm [Aasen 1971; Ballard et al. 2014], see also [Higham 2002] for its analysis. This is different from the blocked Aasen's algorithm [Rozložník et al. 2011] implemented in LAPACK, and the bound on the backward error depends linearly on the tile size. At each step, the algorithm first updates the panel in a left-looking fashion. To exploit the limited parallelism for updating each tile of the panel, PLASMA applies a parallel reduction and accumulates a set of independent updates into a user-supplied workspace. How much parallelism the algorithm can exploit depends on the number of tiles in the panel and the amount of the workspace provided by the user. Once the update is completed, the panel is factorized using the LU panel factorization routine. Hence, the algorithm follows the task dependencies by columns in the nested fashion, as described in the previous section.

Then, in the second stage of the algorithm, the band matrix is factored using the PLASMA band LU factorization routine. Since there is no explicit global synchronization, a task to factor the band matrix can be started as soon as all

```

625 double *a00, *a20;
626 a00 = A(k, k);
627 a20 = A(A.mt-1, k);
628
629 int ma00k = (A.mt-k-1)*A.mb;
630 int na00k = plasma_tile_nmain(A, k);
631 int lda20 = plasma_tile_mmain(A, A.mt-1);
632
633 int nvak = plasma_tile_nview(A, k);
634 int mvak = plasma_tile_mview(A, k);
635 int ldak = plasma_tile_mmain(A, k);
636
637 int num_panel_threads = imin(plasma->max_panel_threads,
638                             minmnt-k);
639 #pragma omp task depend(inout:a00[0:ma00k*na00k]) \
640                       depend(inout:a20[0:lda20*nvak]) \
641                       depend(out:ipiv[k*A.mb:mvak]) \
642                       priority(1)
643 {
644     volatile int *max_idx = (int*)malloc(num_panel_threads*sizeof(int));
645     volatile double *max_val = (double*)malloc(num_panel_threads*sizeof(double));
646     volatile int info = 0;
647
648     plasma_barrier_t barrier;
649     plasma_barrier_init(&barrier);
650
651     #pragma omp taskloop untied shared(barrier) \
652                       num_tasks(num_panel_threads) \
653                       priority(2)
654     for (int rank = 0; rank < num_panel_threads; rank++) {
655         {
656             plasma_desc_t view =
657                 plasma_desc_view(A,
658                                 k*A.mb, k*A.nb,
659                                 A.m-k*A.mb, nvak);
660
661             core_dgetrf(view, &ipiv[k*A.mb], ib,
662                        rank, num_panel_threads,
663                        max_idx, max_val, &info,
664                        &barrier);
665         }
666     }
667     #pragma omp taskwait
668
669     free((void*)max_idx);
670     free((void*)max_val);
671
672     for (int i = k*A.mb+1; i <= imin(A.m, k*A.mb+nvak); i++)
673         ipiv[i-1] += k*A.mb;
674 }

```

Fig. 9. Implementation of the LU panel factorization based on nested tasks with priorities. The `plasma_desc_view` function creates a descriptor for a submatrix, using the original memory of the parent matrix. The `ipiv` array stores the indices of rows for permutation due to pivoting.

the data dependencies are satisfied. This allows the execution of these two algorithms to be merged, improving the parallel performance, especially since both algorithms have limited amount of parallelism that can be exploited. [A more detailed description and performance analysis of the algorithm can be found in \[Yamazaki et al. 2018\].](#)

```

677 double *a00 = A(k, k);
678 for (int m = k+1; m < A.mt-1; m++) {
679     double *amk = A(m, k);
680     #pragma omp task depend (in:amk[0]) \
681         depend (inout:a00[0])
682     { // Some useless work is done here.
683         int l = 1;
684         l++;
685     }
686 }

```

Fig. 10. An example of dummy tasks introduced for creating dependency of a panel starting at address $A(k, k)$ on all its tiles $A(m, k)$.

Name	Description
[zc ds]gesv	linear system solve
[zc ds]posv	positive definite linear system solve

Table 7. Mixed precision routines

2.5 Mixed Precision

PLASMA implements mixed precision routines for the solution of general linear systems of equations and SPD systems of equations. PLASMA mixed precision routines are algorithmically equivalent to their LAPACK counterparts. Table 7 lists all the mixed precision routines implemented in PLASMA.

The algorithms are based on factorizing the matrix in reduced precision (32 bits) and recovering the full precision accuracy (64 bits) in the process of iterative refinement. The approach is motivated by the performance advantage of single precision arithmetic over double precision arithmetic, which is typically twofold. If the input matrix is well conditioned, and the full precision can be recovered in a few steps of refinements, double precision solution can be delivered almost at the speed of computing the single precision solution [Baboulin et al. 2009; Buttari et al. 2007; Langou et al. 2006].

Algorithm 3 summarizes the iterative refinement method in mixed precision for SPD matrices implemented in PLASMA. Dotted quantities \dot{A} , \dot{L} , \dot{x} , \dot{y} , \dot{b} , \dot{d} , \dot{r} denote values in single precision. Adding and removing a dot to a vector corresponds to conversion from double to single precision and vice versa. In order for the algorithm to calculate a residual, a copy of the matrix in full precision needs to be preserved. This incurs additional memory requirements.

In case the refinement procedure does not converge (i.e. backward error stopping criterion is not met) after 30 iterations, the routine falls back to solving the system with a standard algorithm in full precision.

2.6 Matrix Inversion

PLASMA contains a set of routines for computing the inverse of a matrix. Routines for inverting general matrices rely on the LU factorization with partial (row) pivoting, whilst routines for inverting SPD matrices rely on the Cholesky factorization, see Algorithms 4 and 5. The inversion routines are split into three phases: the factorization of the matrix into triangular factors, the inversion of a triangular factor, and the reconstruction of the inverse from its factor.

In general, matrix inversion should not be used for solving linear systems of equations for stability reasons. Instead, matrix factorizations such as LU, LL^T or LDL^T should be used, followed by forward and backward substitution. Yet,

Algorithm 3: Iterative refinement procedure for solution of linear system $Ax = b$ with an SPD matrix A in mixed precision (plasma_dsposv)

Data: A, b
Result: x
 $\dot{A} = \dot{L}\dot{L}^T$ Factorize \dot{A} using Cholesky algorithm, plasma_pspotrf;
 $\dot{L}\dot{y} = \dot{b}$ Solve linear system, plasma_pstrsm;
 $\dot{L}^T\dot{x} = \dot{y}$ Solve linear system, plasma_pstrsm;
 $r = b - Ax$ Compute residual, plasma_pdsymm;
if $\|r\|_{\max} \geq \|x\|_{\max} \|A\|_{\infty} \varepsilon \sqrt{n}$ **then**
 $x_1 = x$ Save computed solution;
 repeat
 $\dot{L}\dot{y} = r_i$ Solve linear system for vector \dot{y} , plasma_pstrsm;
 $\dot{L}^T\dot{d}_i = \dot{y}$ Solve linear system for vector \dot{d} , plasma_pstrsm;
 $x_{i+1} = x_i + d_i$ Update computed solution, plasma_pdgeadd;
 $r_{i+1} = b - Ax_{i+1}$ Compute residual, plasma_pdsymm;
 until $\|r_{i+1}\|_{\max} < \|x_{i+1}\|_{\max} \|A\|_{\infty} \varepsilon \sqrt{n}$;
end

Name	Description
□getri	matrix inversion (LU factorization as input)
□potri	positive definite matrix inversion (Cholesky factorization as input)
□geinv	matrix inversion (includes the LU factorization)
□poinv	positive definite matrix inversion (includes the Cholesky factorization)

Table 8. Matrix inversion routines.

Algorithm 4: Cholesky-based computation of A^{-1} (plasma_omp_dpoinv)

Data: A
Result: A^{-1}
 $A = LL^T$ Cholesky factorization of matrix A , plasma_pdpotrf;
 L^{-1} inverse of L , plasma_pdttrtri;
 $A^{-1} = (L^T)^{-1}L^{-1}$ multiplication of the triangular parts, plasma_pdlauum;

finding the explicit inverse of a matrix is still required in some applications, such as inverting the covariance matrix in statistics.

Table 8 lists all the matrix inversion routines implemented in PLASMA. The poinv function uses the Cholesky factorization (potrf) for finding the inverse of a positive definite matrix (Algorithm 4). This function was introduced to PLASMA to allow overlapping between the three phases of the inversion using the asynchronous tasks. By contrast, the potri function does not include the Cholesky factorization, and it expects a Cholesky factor as input. Similarly, the new geinv function for computing the inverse of a general matrix computes the LU factorization (Algorithm 5), whereas the traditional getri function expects LU factors as input.

Merging the individual stages is known to lead to high performance implementations [Agullo et al. 2010; Bouwmeester and Langou 2010], and it provides very compact traces.

Algorithm 5: LU-based computation of A^{-1} (plasma_omp_dgeinv)

Data: A **Result:** A^{-1} $PA = LU$ LU factorization of matrix A , plasma_pdgetrf; U^{-1} inverse of U , plasma_pdttri; $\tilde{A}^{-1}L = U^{-1}$ find A^{-1} as the solution to a linear system of equations, plasma_pdgetri_aux; $A^{-1} = \tilde{A}^{-1}P$ column permutation of \tilde{A}^{-1} , plasma_pdgeswp;

2.7 Least Squares

PLASMA contains routines for solving overdetermined and underdetermined systems of linear equations. It uses QR and LQ factorizations, based on block Householder transformations. PLASMA implementations are rather different from LAPACK. While LAPACK reduces the input matrices by columns, PLASMA does so by tiles. This approach produces algorithms with higher levels of parallelism and excellent scheduling properties [Buttari et al. 2008, 2009]. Generally, PLASMA QR and LQ algorithms show exceptional *strong scaling*, while being somewhat handicapped in *asymptotic performance*, due to reliance on more complex serial kernels than simple calls to BLAS.

Table 9 lists all the PLASMA routines related to solving overdetermined and under-determined systems of linear equations. This includes routines for QR and LQ factorizations, generation of the Q matrices, as well as application of the orthogonal transformations without explicit generation of the Q matrices.

PLASMA routines have the same numerical stability as LAPACK, but are not algorithmically equivalent to LAPACK. This is because PLASMA reduces the input matrices by tiles, not by full columns, and generates sets of tile reflectors in the process. This makes no difference to the user, as long as PLASMA functions are used for operations involving the reflectors, such as generation of the Q matrix or application of the transformations to another matrix.

PLASMA includes support for QR factorization of tall and skinny matrices, for which the number of rows m is much larger than the number of columns n . In this scenario, algorithmic parallelism is increased by concurrent elimination of blocks within a panel, and proceeds according to a reduction tree until all tiles below the diagonal are eliminated. The approach was described in [Demmel et al. 2008], and extended e.g. in [Dongarra et al. 2013]. Tree-based Householder reductions were recently used for singular value decomposition (SVD) in [Faverge et al. 2016].

Since different trees may be beneficial in different circumstances, PLASMA 17 has introduced several trees and a new flexible implementation of this functionality. A tree is first traversed and the elimination kernels are registered into a 1D array. After this, tasks are created following the order given by this array. This approach permits a quick reuse of a certain tree across all QR and LQ routines as well as the possibility to apply Householder reflectors to form an action of Q or its transpose.

The QR and LQ algorithms are the basis for solving systems with rectangular matrices – the least squares problems for $m \geq n$, and the underdetermined systems for $m < n$. The structure of the plasma_omp_dgels routine is in Algorithm 6. In addition, the QR and LQ factorizations are performed either by the standard algorithms in plasma_pdgeqrf (see Fig. 11) and plasma_pdgelqf, or by their versions based on the reduction tree plasma_pdgeqrf_tree and plasma_pdgelqf_tree. QR algorithm requires custom kernels core_omp_dtsqrt and core_omp_dtsmqt for QR factorization and Q^T application of a matrix composed from two tiles. Although the tile QR factorization (core_omp_dgeqrt) and Q^T application (core_omp_dormqr) correspond to their LAPACK counterparts, inner blocking with block size ib is performed inside these kernels and nonblocked implementations from LAPACK are called.

	Name	Description
833	<code>□gelqf</code>	LQ factorization
834	<code>□gelqs</code>	minimum norm solve using LQ factorization
835	<code>□gels</code>	overdetermined or underdetermined linear systems solve
836	<code>□geqrf</code>	QR factorization
837	<code>□geqrs</code>	least squares solve using QR factorization
838	<code>□[un or]glq</code>	generate the Q matrix from LQ factorization
839	<code>□[un or]gqr</code>	generate the Q matrix from QR factorization
840	<code>□[un or]mlq</code>	apply the Q matrix from LQ factorization
841	<code>□[un or]mqr</code>	apply the Q matrix from QR factorization

Table 9. Least squares routines.

Algorithm 6: Solving overdetermined and underdetermined systems of equations $AX = B$ (`plasma_omp_dgels`)

848 **Data:** A, B
849 **Result:** X
850 **if** $m \geq n$ **then**
851 $A = QR$ QR factorization of A , `plasma_pdgeqrf`;
852 $Y = Q^T B$ application of Q^T to B , `plasma_pdormqr`;
853 $RX = Y$ finding the least-squares solution X , `plasma_pdtrsm`;
854 **else**
855 $A = LQ$ LQ factorization of A , `plasma_pdgelqf`;
856 $LY = B$ solve the linear system for Y , `plasma_pdtrsm`;
857 $X = Q^T Y$ find the minimum norm solution to the underdetermined system, `plasma_pdormlq`;
858 **end**

2.8 Other implementation details.

864 PLASMA is written in C, with interfaces for Fortran provided via automatic code generation during compilation of the
865 library. In particular, PLASMA is shipped with a Python script which parses the C header files, and generates a Fortran
866 module with the interface. The bindings are based on features provided by the Fortran 2003 standard, most importantly
867 the `iso_c_binding` intrinsic module. PLASMA includes several Fortran examples of using the top-level as well as the
868 second-level functions.
869

870 The four different precisions (Table 1) are generated by another Python script. This takes the prototypes in the
871 double complex precision and produces the other precisions by textual substitutions in the source codes.
872

873 Additional details on functionality implemented in PLASMA can be found in [Abalenkovs et al. 2017a].
874

3 PERFORMANCE EVALUATION

876 In this section we present a comprehensive set of benchmarks for the PLASMA routines previously described. Perform-
877 ance is reported for each PLASMA routine on three distinct platforms within a shared memory environment. In each
878 case we utilize the maximum available number of cores and examine performance across a range of matrix sizes. We
879 use real double precision variables throughout, with the exception of the mixed precision routines, which combine real
880 double and real single precision variables. A major focus of this study is to assess the performance of state-of-the-art tile
881 based algorithms, in comparison to block-column based algorithms, such as those present in the LAPACK library.
882
883

18

Dongarra, J. et al

```

885 void plasma_pdgeqrf(plasma_desc_t A, plasma_desc_t T)
886 {
887     for (int k = 0; k < imin(A.mt, A.nt); k++) {
888         int mvak = plasma_tile_mview(A, k);
889         int nvak = plasma_tile_nview(A, k);
890         int ldak = plasma_tile_mmain(A, k);
891
892         core_omp_dgeqrt(mvak, nvak, ib,
893                       A(k, k), ldak,
894                       T(k, k), T.mb);
895
896         for (int n = k+1; n < A.nt; n++) {
897             int nvan = plasma_tile_nview(A, n);
898
899             core_omp_dormqr(PlasmaLeft, PlasmaTrans,
900                           mvak, nvan, imin(mvak, nvak), ib,
901                           A(k, k), ldak,
902                           T(k, k), T.mb,
903                           A(k, n), ldak);
904         }
905         for (int m = k+1; m < A.mt; m++) {
906             int mvam = plasma_tile_mview(A, m);
907             int ldam = plasma_tile_mmain(A, m);
908
909             core_omp_dtsqrt(mvam, nvak, ib,
910                           A(k, k), ldak,
911                           A(m, k), ldam,
912                           T(m, k), T.mb);
913
914             for (int n = k+1; n < A.nt; n++) {
915                 int nvan = plasma_tile_nview(A, n);
916
917                 core_omp_dtsmqr(PlasmaLeft, PlasmaTrans,
918                                A.mb, nvan, mvam, nvan, nvak, ib,
919                                A(k, n), ldak,
920                                A(m, n), ldam,
921                                A(m, k), ldam,
922                                T(m, k), T.mb);
923             }
924         }
925     }
926 }

```

Fig. 11. Skeleton of the standard tile QR factorization. A.mt and A.nt are numbers of rows and columns of tiles in matrix A stored in the tile layout.

3.1 Hardware, Library and Compiler Details

Three recent shared-memory multicore platforms have been selected for this study, namely: a two-socket compute node based on Intel Xeon processors (Haswell generation, 20 cores), an Intel Xeon Phi 7250 processor (Knights Landing generation, 68 cores), and a two-socket machine based on an IBM Power 8 processor (20 cores). Details of the individual platforms are presented in Table 10.

On these three hardware platforms we compare the performance of PLASMA to other numerical libraries. In particular the Netlib LAPACK library version 3.7.0, linked with a multithreaded optimized BLAS library, provides the baseline for performance comparisons. In the case of Intel architectures we also compare the performance of PLASMA against that of the Intel Math Kernel Library (MKL). For the IBM Power 8 based system, the IBM Engineering and Scientific

937 Subroutine Library (ESSL) is used for comparison instead. It should be noted that PLASMA is also linked with these
938 libraries and relies on their sequential implementations of BLAS.

939 For most tests square matrices of growing size are used; however, non-square matrices are also examined where
940 appropriate to the algorithm, such as in the case of QR factorization. For each test, three runs were performed at each
941 matrix size, using randomly generated matrices. The highest performance obtained from these three runs is reported in
942 the plots.
943

944 A crucial parameter within PLASMA is the size of the square tile; i.e., the `nb` parameter. Lower values will typically
945 increase the parallelism of the algorithm, while higher values allow more efficient utilization of arithmetic units.
946 Consequently PLASMA performance is examined for several tile sizes, with the highest performing tile size reported.
947 The optimal tile size tends to grow slightly as the matrix size is increased. **A quick way for users to determine an `nb`
948 parameter suitable for their architecture and matrix size is to run the PLASMA tester on a range of tile sizes, and then
949 set the one that leads to the best performance through a call to the `plasma_set` function.**
950

951 On both the Haswell and Phi platforms, PLASMA and MKL are linked using the GNU C compiler, and utilize the
952 GNU OpenMP (`gomp`) runtime library. Due to issues with using this combination for LAPACK linked with MKL BLAS,
953 we present results for this combination using the Intel C compiler, and the Intel OpenMP (`iomp`) runtime library.
954

955 On the Haswell platform tests are performed using the following options:

```
956 OMP_NUM_THREADS=20 OMP_PROC_BIND=true OMP_MAX_TASK_PRIORITY=100 numactl --interleave=all
```

957 For the Phi platform tests are run using:

```
958 OMP_NUM_THREADS=68 OMP_PROC_BIND=true OMP_MAX_TASK_PRIORITY=100 numactl -m=1
```

959 where the last flag has led to using the fast MCDRAM memory for storing the matrices. **The Phi processor was in the
960 flat memory mode, allowing the allocation of large matrices in the MCDRAM memory. This had a significant effect on
961 performance compared to allocating matrices in RAM. The quadrant cluster mode was used, although this did not seem
962 to have a significant impact on performance. The effect of the different memory modes of Phi on performance for linear
963 algebra has been studied in more detail in [Haidar et al. 2017].**
964

965 POWER8 runs use the following:

```
966 OMP_NUM_THREADS=20 OMP_PROC_BIND=true OMP_PLACES="{0}:20:8" OMP_MAX_TASK_PRIORITY=100
```

967 where the
968 `OMP_PLACES` environment variable maps each OpenMP thread to one physical CPU core, rather than simply taking the
969 first 20 available logical cores.
970

971 We present an execution trace for the Cholesky-based matrix inversion. Many more traces can be found in [Abalenkovs
972 et al. 2017b].
973

974 3.2 Parallel BLAS

975 PLASMA contains a full parallel implementation of the Level 3 BLAS routines. However, this section focuses only on
976 the performance results of `gemm` and `trsm`. This is motivated by the fact that all level 3 BLAS routines, except `trsm`, can
977 be viewed as a specialized implementation of `gemm` [Kågström et al. 1998].
978

979 We present the performance of `plasma_dgemm` and `plasma_dtrsm` routines on three different architectures, and
980 compare it with the performance of the vendor-provided optimized implementations. Unlike LAPACK routines we do
981 not report the performance of the Netlib reference implementation of BLAS, as it is fully sequential.
982

983 Figures 12 and 13 show the performance results on Haswell. For the `dgemm` routine, MKL performs about 15% better
984 than PLASMA throughout the range of matrix sizes. This result suggests that the current `plasma_dgemm` routine may
985

Label	Hardware overview	Compilers and libraries
Haswell	<ul style="list-style-type: none"> • 2× Intel Xeon CPU E5-2650 v3, 2.30GHz • 2×10 = 20 cores • 32 GB DRAM • theoretical peak performance 736 Gflop/s 	<ul style="list-style-type: none"> • GNU Compiler Collection (GCC) 7.1.0 • Intel C Compiler 16.0.3 • MKL 17.2
Phi	<ul style="list-style-type: none"> • Intel Xeon Phi 7250 • 68 cores • 16 GB MCDRAM • theoretical peak performance 3046 Gflop/s • quadrant cluster mode • flat memory mode 	<ul style="list-style-type: none"> • GNU Compiler Collection (GCC) 7.0.1 • Intel C Compiler 16.0.3 • MKL 17.2
POWER8	<ul style="list-style-type: none"> • 2× IBM POWER8, 3.5GHz • 2× 10 = 20 cores • 256 GB DRAM • theoretical peak performance 560 Gflop/s 	<ul style="list-style-type: none"> • GNU Compiler Collection (GCC) 6.3.1 • IBM XL 20161123 • IBM ESSL 5.5.0

Table 10. Platforms selected for the benchmarks.

have potential room for performance improvement. For the `plasma_dtrsm` routine, PLASMA provides performance similar to MKL, whilst offering a more smooth and predictable performance scaling.

The results on the Phi architecture (Figs. 14 and 15) demonstrate that MKL is making significantly better use of the 68 available cores. For moderate-sized matrices; i.e. in the 2000 to 10000 range, a performance gap of around 500 Gflop/s can be observed for `dgemm`. For `dtrsm` the performance gap is consistently around 200 Gflop/s. **These results suggest a significant deficit in efficiency for the PLASMA BLAS routines, in comparison to multithreaded MKL, despite the fact that PLASMA calls sequential MKL BLAS for processing individual tiles.**

On the IBM POWER8 platform, PLASMA and the vendor optimized multithreaded library, ESSL, exhibit comparable results for both `dgemm` and `dtrsm`. As shown in Figs. 16 and 17, both routines reach in excess of 450 Gflop/s, representing around 85% of the theoretical peak performance (560 Gflop/s). This result demonstrates the capability of PLASMA to efficiently exploit all 20 cores of the POWER8 machine. **Again, PLASMA tasks call sequential `dgemm` from ESSL to process individual tiles.**

The optimal tile size parameter (`nb`) was either 336 or 560 on Haswell, for matrices larger than 4000. The optimal size was 560 on Phi, and 384 on POWER8. Smaller matrices require somewhat smaller tiles for optimal performance.

3.3 Parallel Norms

We present benchmarks for computation of the *one* norm, for general and symmetric matrices; i.e., the `dlange` and `dlansy` routines respectively. These routines are heavily memory bound; hence, their performance is reported in GB/s rather than Gflop/s.

Results on Haswell are summarized in Figs. 18 and 19. For both general matrices (Fig.18), and symmetric matrices (Fig. 19), MKL significantly out-performs PLASMA and LAPACK. It should be noted that the high performance of MKL was obtained only after calling the C interface function without the ‘not a number’ (NaN) checking; namely, the

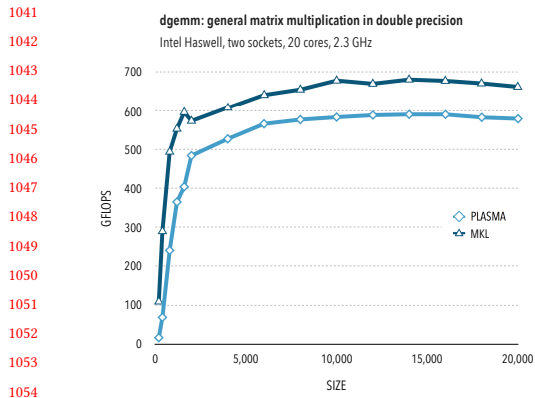


Fig. 12. Performance of dgemm on Haswell.

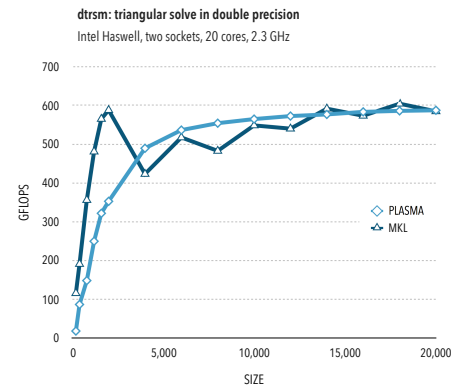


Fig. 13. Performance of dtrsm on Haswell.

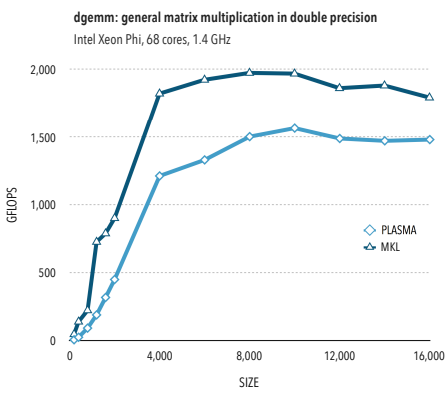


Fig. 14. Performance of dgemm on Phi.

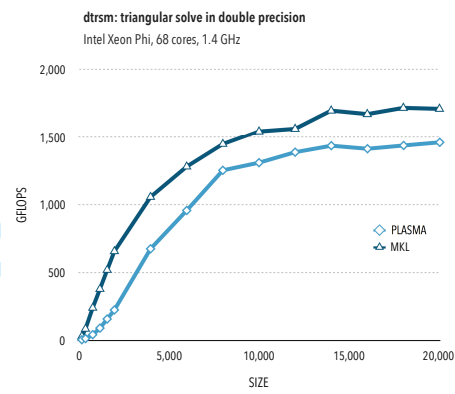


Fig. 15. Performance of dtrsm on Phi.

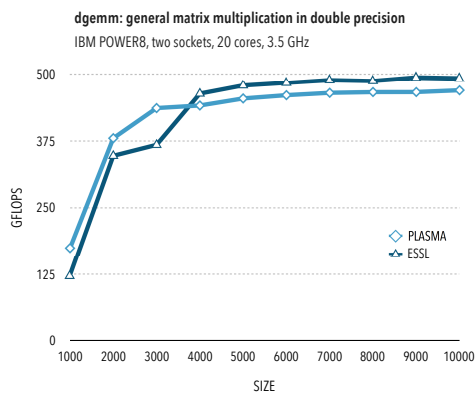


Fig. 16. Performance of dgemm on POWER8.

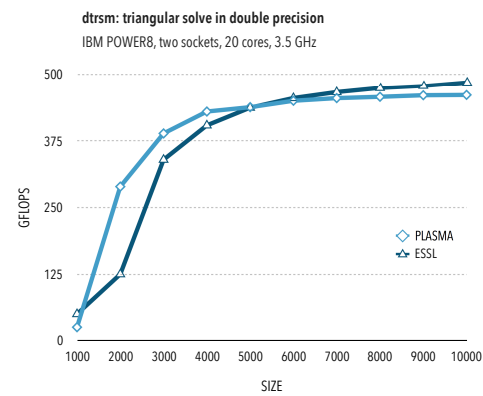


Fig. 17. Performance of dtrsm on POWER8.

LAPACKE_dlange_work and LAPACKE_dlansy_work. With LAPACKE_dlange and LAPACKE_dlansy, the performance was significantly worse. In this benchmark, PLASMA is penalized due to the inclusion of translation to the tile layout into the measured time, since this conversion significantly increases the number of memory accesses required. To quantify this effect, we have also performed an experiment excluding the layout conversion from the timing. These results are denoted as ‘PLASMA*’ (with asterisk) in the plots. We can see that if the matrix is already in the tile layout, the norm computations can be performed even faster than by MKL.

The results on the Phi platform are presented in Figs. 20 and 21. As in the case of Haswell, MKL significantly outperforms both PLASMA and LAPACK, with the performance differential growing significantly with increasing matrix size. The increased parallelism of the Phi platform does allow PLASMA to significantly out-perform LAPACK however. We have repeated the experiment excluding the layout conversion time of PLASMA also on Phi. In this scenario, MKL still performs better for general matrices, while PLASMA outperforms MKL for symmetric ones.

Results obtained on the POWER8 platform are shown in Figs. 22 and 23. For both general and symmetric matrices, PLASMA out-performs ESSL by around 50%, and offers roughly twice the performance of LAPACK.

The dominant optimal tile size parameter (nb) was found to be 560 on Haswell, 1024 on Phi, and 384 on POWER8.

3.4 Linear Systems

The PLASMA library provides a range of routines for the factorization of matrices. In this section we examine performance for the PLASMA implementations of LU factorization (`plasma_dgetrf`), Cholesky factorization (`plasma_dpotrf`), and LDL^T factorization (`plasma_dsytrf`) with dense matrices. We also consider performance for the band-matrix versions of LU and Cholesky factorization; i.e. (`plasma_dgbtrf`) and (`plasma_dpbtrf`). The performance of QR factorization routines for solving least squares problems are presented in Section 3.7.

We consider first the performance of PLASMA on the Haswell platform. For LU factorization (Fig. 24), MKL shows a moderate performance gain over PLASMA throughout the range of matrix sizes, at around 15%. PLASMA does significantly outperform LAPACK however, showing around a 50% improvement. This improvement is partially due to the parallel panel factorization of PLASMA, in contrast to the standard LU algorithm of LAPACK, which introduces parallelism only through parallel BLAS used for the trailing matrix update.

Fig. 25 shows the performance of Cholesky factorization. Here PLASMA and MKL offer very similar performance, with MKL slightly faster for small matrices, and PLASMA slightly ahead for mid-sized matrices. Both MKL and PLASMA again offer significantly improved performance over LAPACK.

Results for the LDL^T factorization are shown in Fig. 26. While LU and Cholesky factorization shows a high performance up to 600 Gflop/s, which is around 80% of the theoretical peak performance (see Table 10), none of the `dsytrf` implementations achieve even 50% of the theoretical peak. The bottlenecks to providing a scalable implementation of the symmetric indefinite matrix have been discussed in Section 2.4.3; the main issue being the need for symmetric pivoting. Nevertheless, PLASMA is able to outperform MKL and LAPACK by significant margin, for moderate to large matrices.

Results on the Phi platform are shown in Figs. 27–29. Overall trends are very similar to Haswell; in particular for the LU and Cholesky algorithms. In the case of LDL^T factorization, PLASMA outperforms MKL by a more significant margin than on Haswell, offering more than double the performance on larger matrices.

On the IBM POWER8 architecture, both the ESSL and PLASMA implementations of LU factorization substantially outperform the LAPACK equivalent, as showed in Fig. 30. For smaller matrices ESSL demonstrates good performance relative to PLASMA; however it stagnates early whilst PLASMA performance continues to grow with increasing

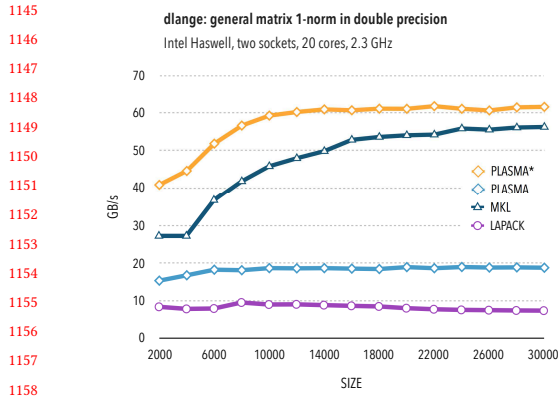


Fig. 18. Performance of dlange on Haswell.

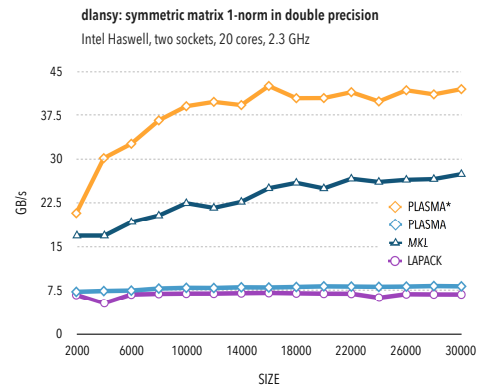


Fig. 19. Performance of dlansy on Haswell.

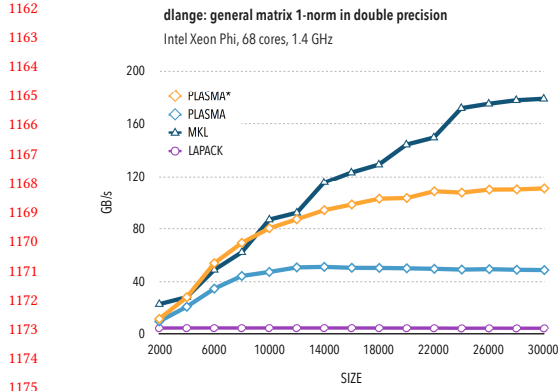


Fig. 20. Performance of dlange on Phi.

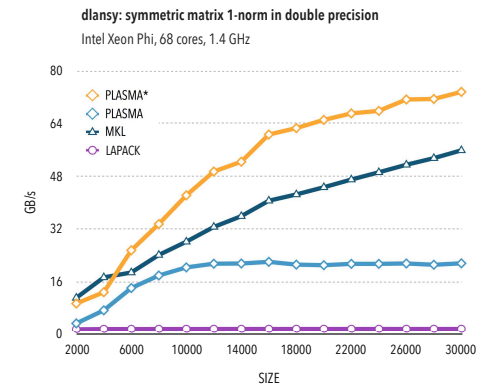


Fig. 21. Performance of dlansy on Phi.

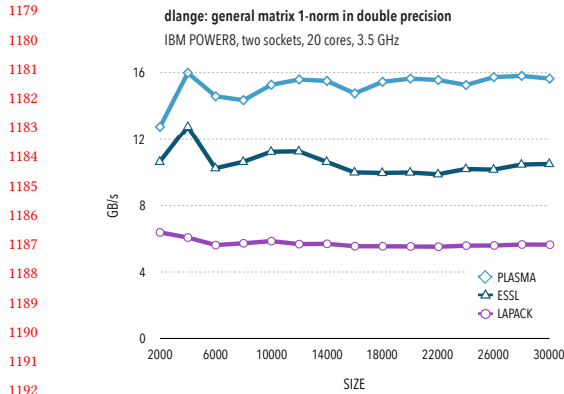


Fig. 22. Performance of dlange on POWER8.

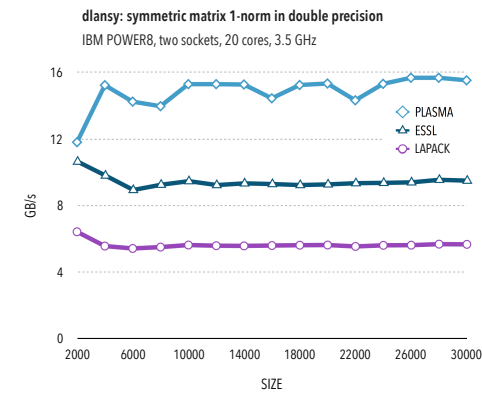


Fig. 23. Performance of dlansy on POWER8.

1197 matrix sizes. The POWER8 experiments for Cholesky factorization; Fig. 31, show ESSL and PLASMA achieving similar
1198 performance for smaller matrices, while PLASMA pulls ahead by around 25% for moderately large matrices.

1199 The results for LDL^T factorization arise more curiosity. For matrices of size ranging from 1000 to 5000, the three
1200 curves completely overlap, which suggests that either for such small matrices there is no much room for parallelism
1201 exploitable by the LDL^T algorithm, or ESSL and PLASMA failed to achieve a better optimization than LAPACK. The
1202 latter is more true for ESSL that did not succeed in showing any performance gain over LAPACK for all the matrix sizes
1203 considered. On the other hand, the performance of PLASMA's LDL^T , increased almost linearly, with the matrix size.

1204 To examine the performance of band routines we consider the `dgbrtf` and `dpbtrf` functions, which employ LU and
1205 Cholesky factorization respectively, to solve the band systems. In each case we consider a matrix with a 10 percent
1206 band occupancy; that is, the bandwidth is equal to one tenth of the matrix size.

1207 Figures 33 and 34 show the performance of the band routines on the Haswell platform. For Cholesky factorization
1208 (Fig. 34) we see a very similar performance profile across all three platforms; however, with LU factorization (Fig. 33)
1209 PLASMA pulls ahead of MKL and LAPACK for large matrix sizes, showing up to a 100% increase in performance over
1210 MKL. The improved relative performance of PLASMA in this case appears to be a result of the multi-threaded panel
1211 factorization.

1212 Performance on the Xeon Phi is shown in Figs. 35 and 36. Here performance with LU is similar between PLASMA
1213 and MKL; PLASMA offers better performance on large matrix sizes, with MKL ahead for small matrices. For Cholesky
1214 all three routines provide similar performance with smaller matrices, while PLASMA offers increasingly superior
1215 performance as the matrix size grows.

1216 The results on POWER8, given in Figs. 37 and 38, show significant performance improvements for PLASMA over
1217 LAPACK and ESSL throughout the range of matrix sizes, on both routines. The difference is particularly evident for LU
1218 factorization, where PLASMA performance grows to more than double that of the other routines at large matrix sizes.

1219 It is important to note that, for band routines in general, performance will scale much more strongly with bandwidth
1220 than with matrix size. Increasing the matrix size whilst using a fixed bandwidth of modest size will typically provide a
1221 flat performance profile, as memory bandwidth becomes saturated before the floating point capacity is exhausted.

1222 The dominant optimal tile size parameter (`nb`) for Cholesky factorization of a dense matrix was 336 on Haswell, 448
1223 on Phi, and 384 on POWER8. For LU factorization, it was 228 on Haswell, 448 on Phi and 336 on POWER8. Performance
1224 of the LU factorization was found to be sensitive to the maximum number of threads for panel factorization (`mtpf`),
1225 which was set to 8 on Haswell, 20 on Phi, and 4 on POWER8. The inner blocking parameter (`ib`) was set to 16 on
1226 Haswell, 40 on Phi, and 32 on POWER8. Finally, for the LDL^T factorization, the dominant optimal `nb` was found to be
1227 192 on Haswell, 352 on Phi, and 128 on POWER8.

1228 For band Cholesky factorization, the dominant `nb` was 224 on Haswell and Phi, and 128 on POWER8. For band LU
1229 factorization, the dominant optimal `nb` was 168 on Haswell, 224 on Phi and 128 on POWER8. The maximal number of
1230 threads for panel factorization (`mtpf`) was set to 4 on Haswell and POWER8, and to 8 on Phi.

1240 3.5 Mixed Precision

1241 Performance of the mixed precision iterative refinement based on the LU factorization is presented in Figs. 39, 41,
1242 and 43. At the time of writing, an issue is present with the coupling of PLASMA to the `gomp` runtime library version
1243 7. This issue is related to the assignment of priorities for nested OpenMP tasks; an approach employed by the LU
1244 factorization in PLASMA. To circumvent this issue task priorities are not enabled for the presented results; i.e. setting
1245 `OMP_MAX_TASK_PRIORITY=0`. Even with this limitation PLASMA is able to achieve around 25% higher performance than
1246

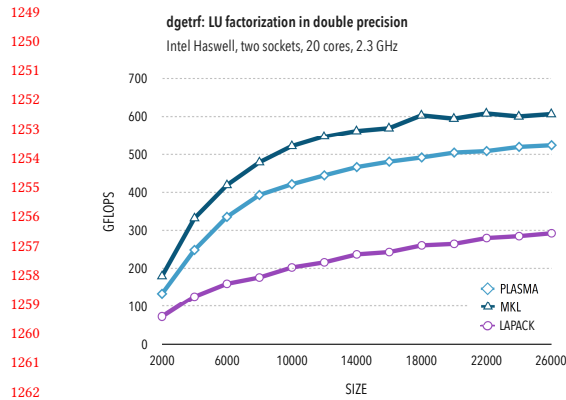


Fig. 24. Performance of dgetrf on Haswell.

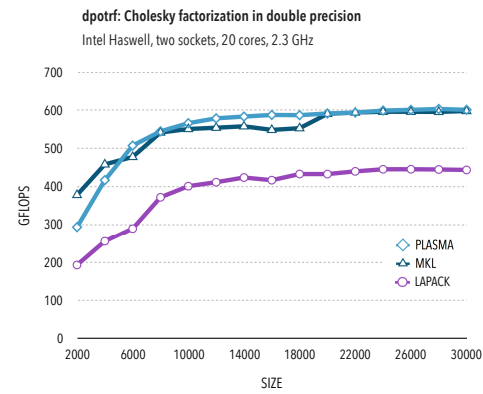


Fig. 25. Performance of dpotrf on Haswell.

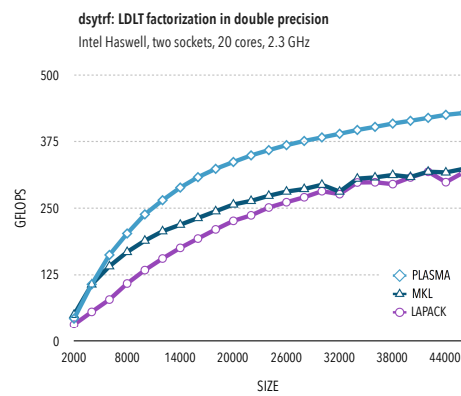


Fig. 26. Performance of dsytrf on Haswell.

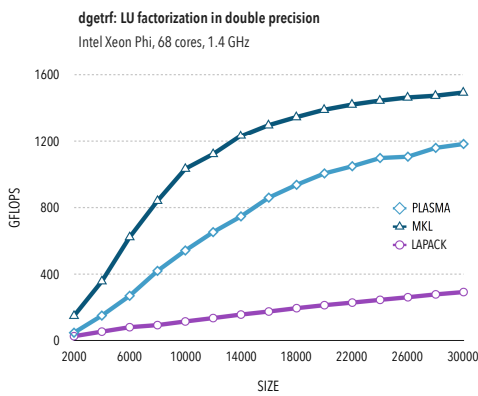


Fig. 27. Performance of dgetrf on Phi.

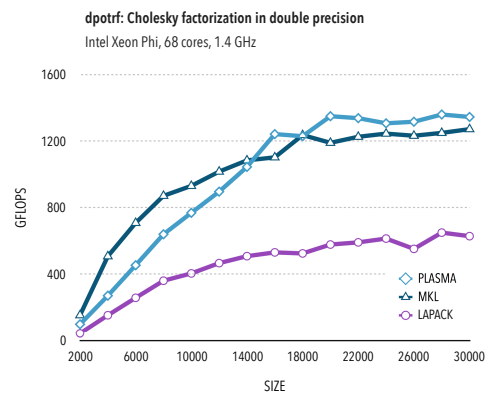


Fig. 28. Performance of dpotrf on Phi.

1301
1302
1303
1304
1305
1306
1307
1308
1309
1310
1311
1312
1313
1314
1315
1316
1317
1318
1319
1320
1321
1322
1323
1324
1325
1326
1327
1328
1329
1330
1331
1332
1333
1334
1335
1336
1337
1338
1339
1340
1341
1342
1343
1344
1345
1346
1347
1348
1349
1350
1351
1352

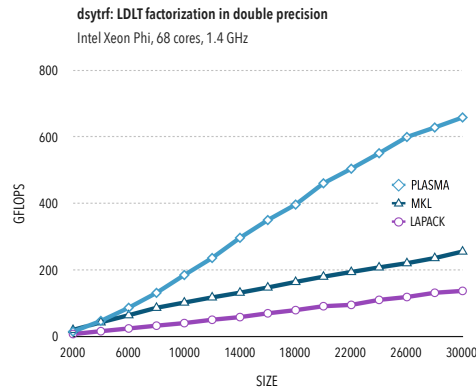


Fig. 29. Performance of dsytrf on Phi.

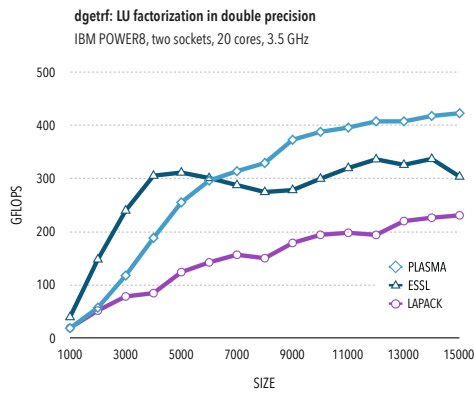


Fig. 30. Performance of dgetrf on POWER8.

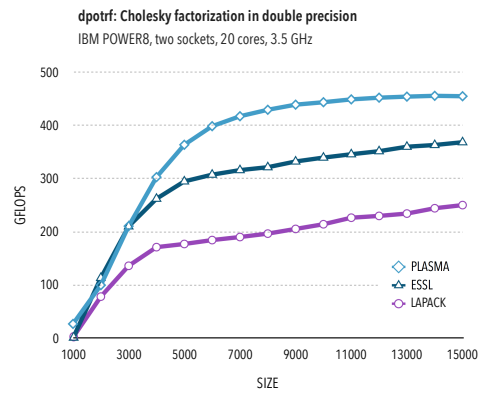


Fig. 31. Performance of dpotrf on POWER8.

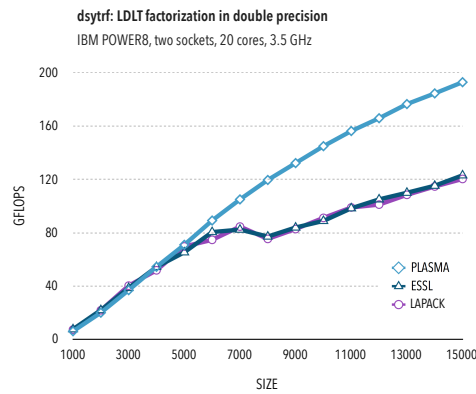


Fig. 32. Performance of dsytrf on POWER8.

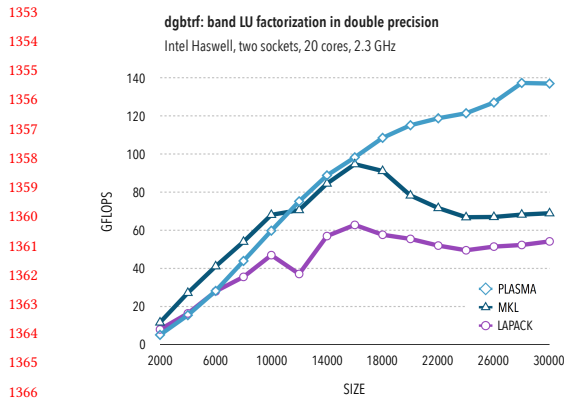


Fig. 33. Performance of dgbrtf on Haswell.

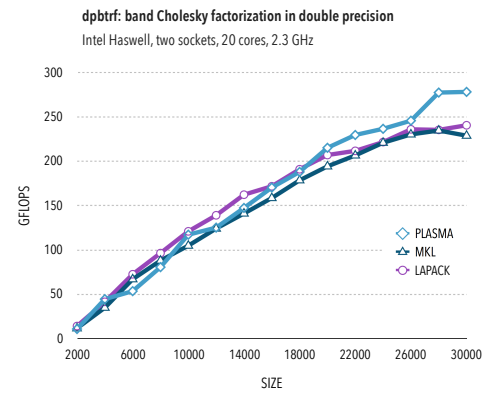


Fig. 34. Performance of dpbrtf on Haswell.

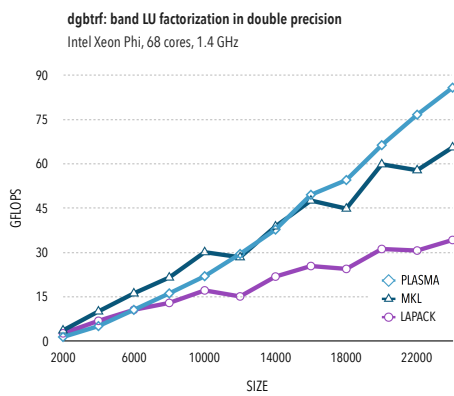


Fig. 35. Performance of dgbrtf on Phi.

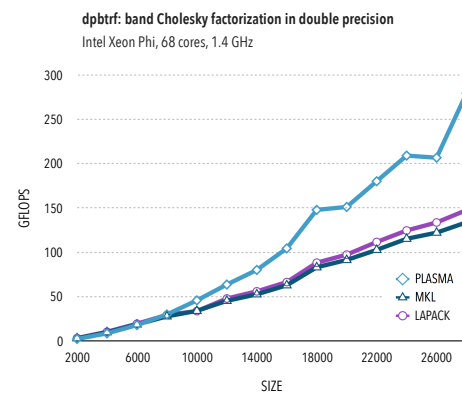


Fig. 36. Performance of dpbrtf on Phi.

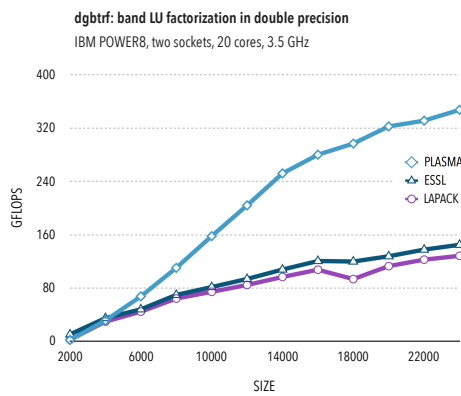


Fig. 37. Performance of dgbrtf on POWER8.

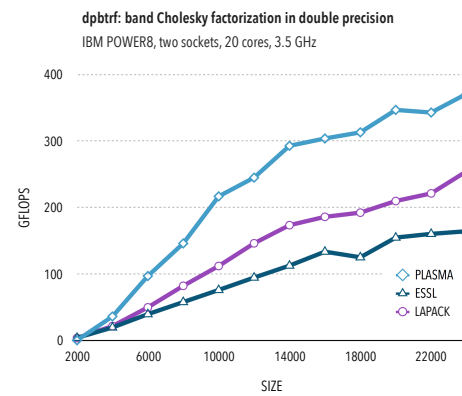


Fig. 38. Performance of dpbrtf on POWER8.

1405 MKL, and more than double the performance of LAPACK on Haswell. On Phi the difference is even more significant;
1406 PLASMA achieves around double the performance of MKL, and around quadruple the performance of LAPACK. On
1407 POWER8 the performance of PLASMA is comparable with that of ESSL. Here PLASMA offers slightly better performance
1408 for smaller matrices, with ESSL slightly ahead for larger matrices. Both libraries provide roughly double the performance
1409 of LAPACK.
1410

1411 Performance results of the mixed precision iterative refinement routine `dsposv`, based on Cholesky factorization, are
1412 presented in Figs. 40, 42, and 44. The number of right hand side vectors is set to one in all experiments. On the Haswell
1413 platform, PLASMA achieves significantly higher performance than MKL for large matrix sizes. On Phi, the PLASMA
1414 routine provides a dramatic four- to five-fold improvement compared to its MKL counterpart, for moderate to large
1415 matrix sizes.
1416

1417 The dominant optimal tile size for the `plasma_dsgesv` routine on Haswell was 384, with inner blocking `ib = 40`,
1418 and 4 threads used for panel factorization. The same setup was used on POWER8. On Phi, tile size was 352, the inner
1419 blocking `ib = 64`, and 8 threads were assigned to panel factorization. Optimal tile sizes for the `plasma_dsposv` routine
1420 were more varied, while being dominated by 480 for Haswell, 576 for Phi, and 384 for POWER8.
1421

1422 Figs. 41 and 42 present two additional curves corresponding to conventional linear system solutions in single and
1423 double precisions, denoted by PLASMA(S) and PLASMA(D) respectively. In order to compare performance of all three
1424 variants of the linear system solution; `s{ge,po}sv`, `d{ge,po}sv` and `ds{ge,po}sv`, the performance for all routines
1425 was calculated using the same formula for the number of floating point operations.
1426

1427 As expected, the mixed precision routine delivers a performance curve that lies between that of the native single and
1428 double precision results. The mixed precision performance curve lies much closer to the single precision results in case
1429 of the `□posv` routine, whereas in case of `□gesv`, performance is more comparable to that of the native double precision
1430 routine.
1431

1432 3.6 Matrix Inversion

1433 The routines used to explicitly invert a matrix are described in section 2.6. The performance results on the various
1434 systems are collated in Figs. 46–51. On the Haswell architecture (Figs. 46 and 47) we see that PLASMA is more
1435 performant than MKL and LAPACK for all matrix sizes. PLASMA is particularly effective for Cholesky inversion, where
1436 performance improvements over MKL are mostly around 50-100%. On the Phi platform (Figs. 48 and 49) the performance
1437 of PLASMA is slightly higher than MKL for `dgeinv`, though PLASMA is once again around twice as fast for `dpoinv`.
1438 For both algorithms the performance of LAPACK is well below that of the more heavily optimized libraries. On the
1439 POWER8 machine (Figs. 50 and 51) things behave rather differently. For `dgeinv` the performance of PLASMA is the
1440 best for matrices larger than around 5000. The `dpoinv` implementation in PLASMA once again provides the fastest
1441 implementation, though by a smaller margin than on the other platforms. Here ESSL is roughly halfway between the
1442 performance of PLASMA and LAPACK.
1443

1444 In summary, for `dgeinv` PLASMA obtains slightly superior performance to MKL on Intel architectures and it is faster
1445 than ESSL for large matrices on the POWER8 system. However, for `dpoinv`, PLASMA significantly outperforms the
1446 other implementations on all systems.
1447

1448 The performance benefit of the `plasma_dpoinv` routine stems from the fact that its tile-based Cholesky factorization
1449 algorithm is well suited for overlapping the factorization with the subsequent stages (see Algorithm 4). The effect is
1450 best shown in an execution trace, see e.g. Fig. 45. It is clear that kernels of the subsequent stages start before the end of
1451 the factorization itself, filling the gaps of the factorization algorithm towards the end of the factorization, where this
1452

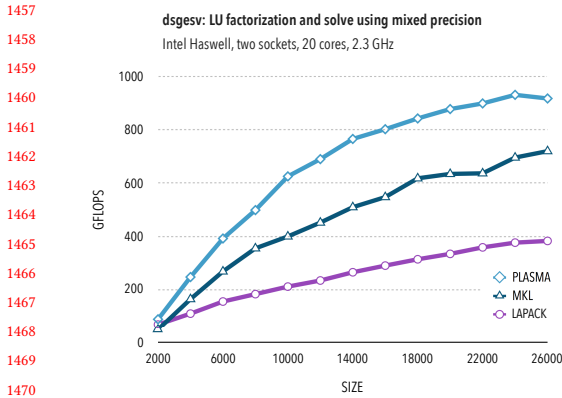


Fig. 39. Performance of dsgesv on Haswell

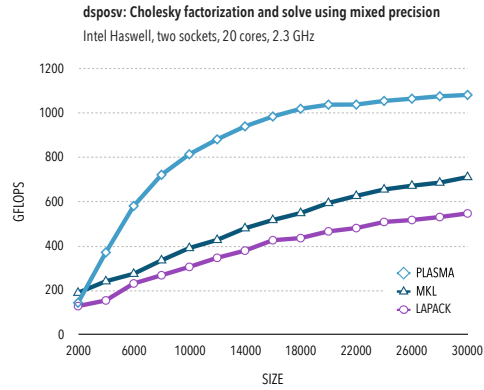


Fig. 40. Performance of dsposv on Haswell

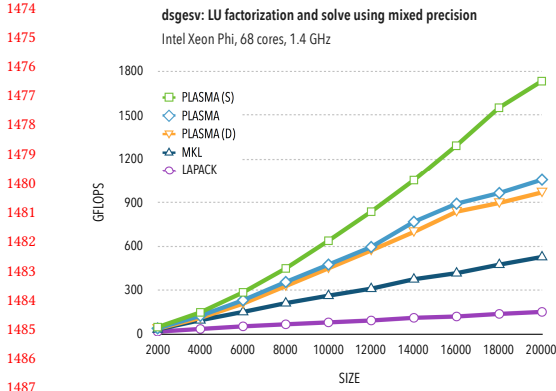


Fig. 41. Performance of dsgesv on Phi

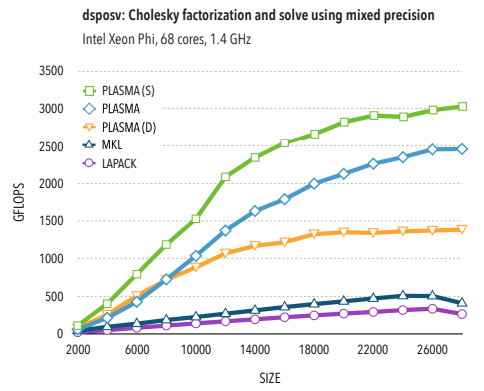


Fig. 42. Performance of dsposv on Phi

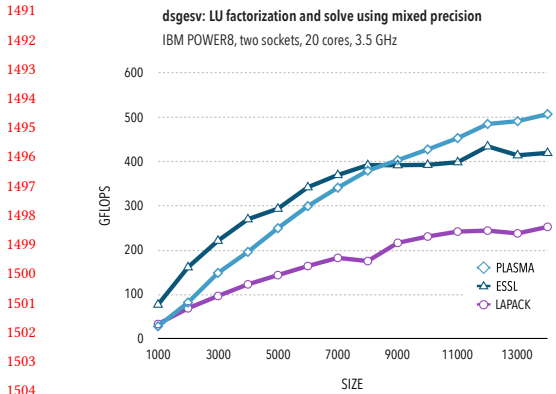


Fig. 43. Performance of dsgesv on POWER8

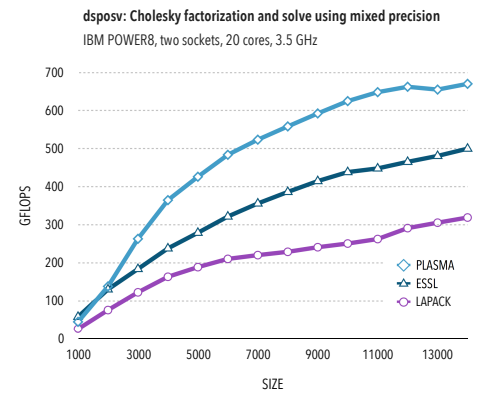


Fig. 44. Performance of dsposv on POWER8

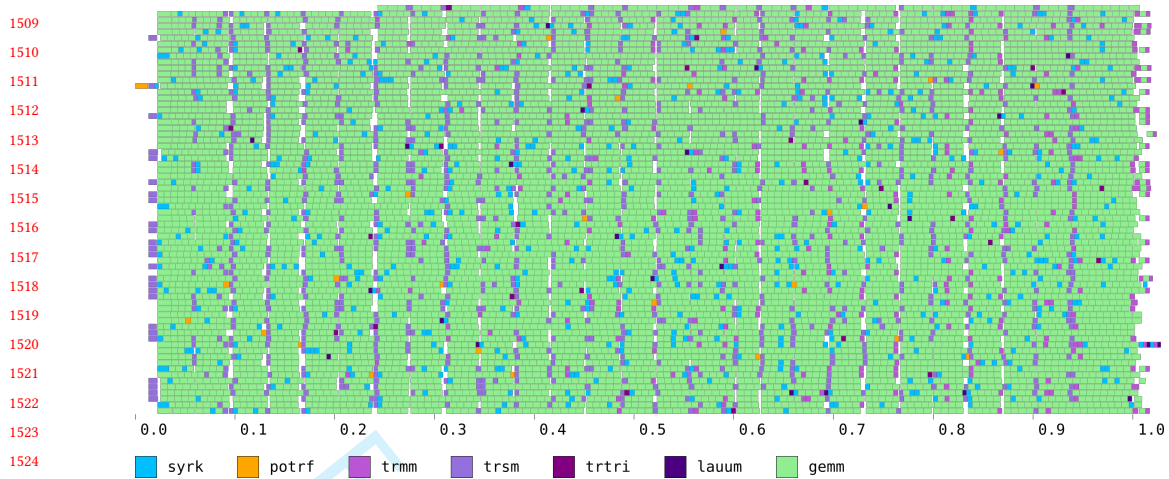


Fig. 45. Trace of plasma_dpoinv on Phi, matrix size 11 648, tile size 448.

does not generate enough parallelism itself. Unfortunately, partial pivoting prevents such a high degree of overlap in the LU-based routine `plasma_dgeinv`.

The optimal tile size parameter (`nb`) did not tend to change much with the matrix size. For the `dgeinv` routine, the dominant optimal `nb` was 384 for Haswell, 448 for Phi, and 256 for POWER8. For the `dpoinv` implementation, the dominant `nb` was 544 on Haswell, 448 on Phi, and 256 on POWER8.

3.7 Least Squares

Solving overdetermined problems in PLASMA relies on the QR factorization of the matrix (see Algorithm 6). We perform the benchmarks for the QR factorization routine (`plasma_dgeqrf`) which allows us to avoid dependence on the number of right hand sides. We run PLASMA using the standard QR algorithm, in which the `plasma_pdgeqrf` function (Figure 11) is called, and also with the tree-based QR algorithm, in which the `plasma_pdgeqrf_tree` function is used instead. In the charts to follow, ‘PLASMA’ (no asterisk) refers to the standard algorithm, while ‘PLASMA*’ (with asterisk) refers to the tree-based one.

Results are summarized in Figs. 52–57. The first experiment is monitoring the performance of the QR factorization on square matrices of increasing dimension. In this scenario, updating the trailing matrix provides enough parallelism to keep the cores busy. As a result, for PLASMA, the tree-based algorithm is providing slightly lower performance than the standard algorithm on all the tested platforms. This is related to the worse data locality due to the need for visiting some tiles twice when eliminating them by the `tt` (triangle-on-top-of-triangle) kernels rather than by the `ts` (triangle-on-top-of-square) kernels, see e.g. [Bouwmeester and Langou 2010] for related discussion. This experiment also suits the MKL library, which is faster than PLASMA by about 15% on Haswell and by more than 30% on Phi. It suits also the ESSL, which is about 10% faster than PLASMA on POWER8. Finally, LAPACK with multithreaded BLAS provides significantly lower performance, which is around 40% of the one by PLASMA on Haswell and Phi, and around 60% for POWER8.

The situation changes significantly if updating the trailing matrix does not provide enough parallelism, which is the case for matrices with $m \gg n$, also called ‘tall and skinny’ in literature. Our second experiment aims at performance

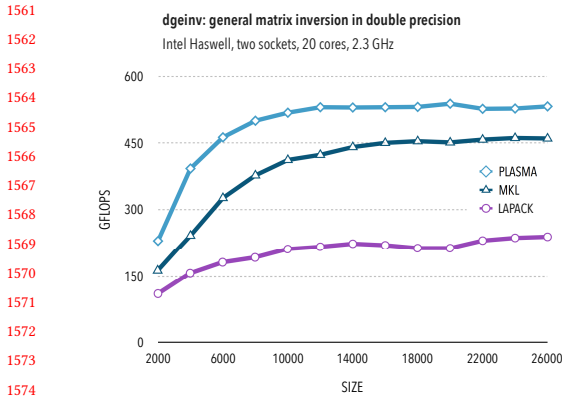


Fig. 46. Performance of dgeinv on Haswell.

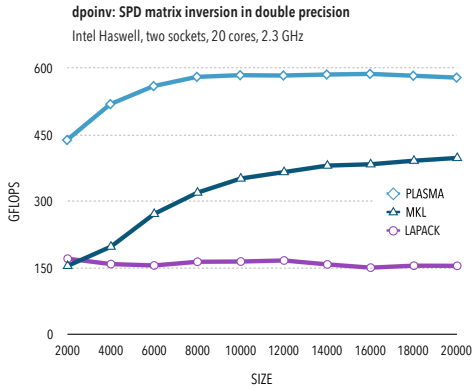


Fig. 47. Performance of dpoinv on Haswell.

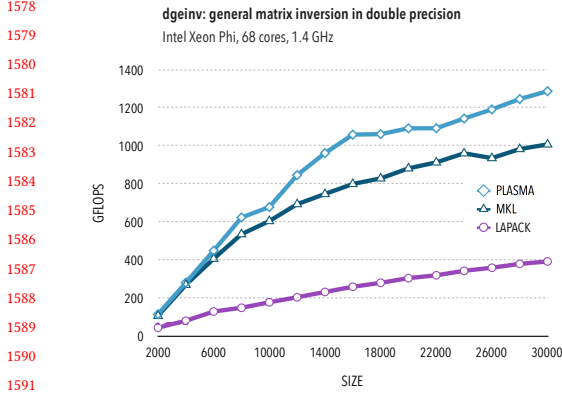


Fig. 48. Performance of dgeinv on Phi.

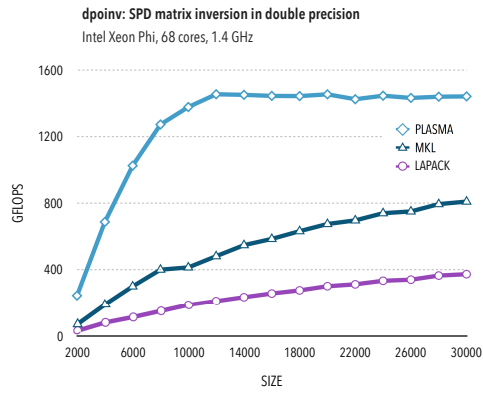


Fig. 49. Performance of dpoinv on Phi.

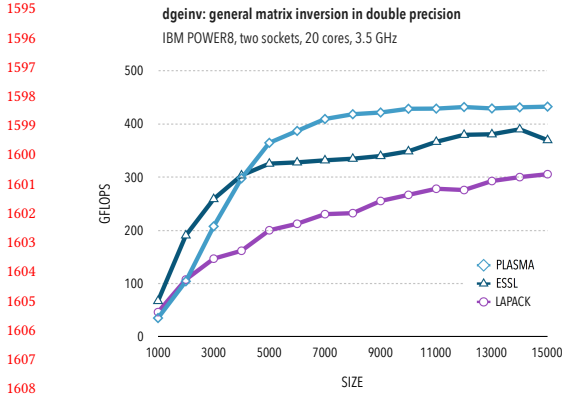


Fig. 50. Performance of dgeinv on POWER8.

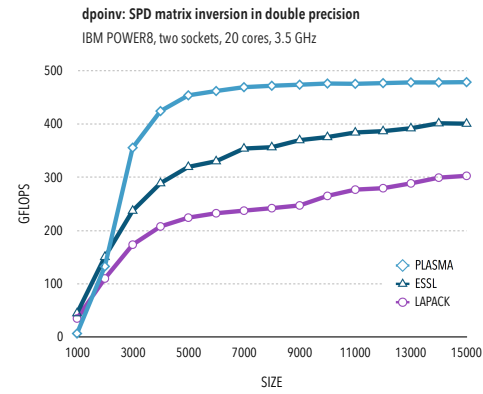


Fig. 51. Performance of dpoinv on POWER8.

1613 of QR factorization for such matrices, in particular, on a matrix with 90 000 rows, and variable number of columns.
1614 In this scenario, it is crucial to introduce parallelism also into elimination of the columns of tiles, as it is done for
1615 the tree-based algorithm of PLASMA. Indeed, this algorithm significantly outperforms the standard algorithm in this
1616 regime. Nevertheless, for increasing number of matrix columns, the standard algorithm gets enough parallelism and
1617 reaches the performance of the tree-based elimination. In our experiments, this has happened already for 8 columns
1618 of tiles. LAPACK results follow the trend of the standard PLASMA algorithm, not having parallelism for very skinny
1619 matrices and resembling the results for square matrices for increasing number of columns.
1620

1621 A somewhat surprising performance profile was provided by MKL for this experiment. On Haswell (Fig. 53), the initial
1622 performance for matrix with 300 columns is almost as high as for the tree-based PLASMA algorithm, suggesting that
1623 MKL also introduces some parallelism into the panel elimination. However, the performance does not increase for larger
1624 matrices, and it got even lower than for LAPACK for the case with 9600 columns. On Phi however, the performance of
1625 MKL started as low as for the standard PLASMA algorithm, while keeping higher than it for more columns, consistently
1626 with the square-matrix results. Performance of ESSL on POWER8 starts between the two PLASMA algorithms, while
1627 being lower between 1200 and 4800 columns, and matching them for the case with 9600 columns.
1628

1629 The performance of PLASMA is not particularly sensitive to the tile size parameter (nb) on Haswell, with most of the
1630 results obtained using nb = 288. The dependence was stronger on Phi, with 448 and 560 being the optimal values for
1631 larger matrices. The results on POWER8 were obtained with nb = 336. The ib parameter for inner blocking inside the
1632 kernels for QR factorization has been consistently set to ib = nb/4 on Haswell and Phi, while it has been set to 64 on
1633 POWER8.
1634

1635 4 CONCLUSIONS

1636 During the latest major revision of PLASMA, the library has been ported from an in-house developed runtime system;
1637 QUARK, to OpenMP tasks with dependencies. While QUARK has features specific to the needs of a numerical library,
1638 OpenMP is a more general purpose tool. Consequently, the transition has also led to the redesigning of some algorithms;
1639 most notably the LU factorization code.
1640

1641 A comprehensive set of performance benchmarks has been performed, considering three recent multicore shared
1642 memory architectures, namely Haswell, Xeon Phi, and POWER8. In general, the performance of PLASMA is comparable
1643 to the optimized vendor libraries; Intel MKL in the case of Intel architectures, and IBM ESSL for POWER8. In addition,
1644 the LAPACK library using multithreaded BLAS from the vendor optimized library has been also included for the
1645 comparison.
1646

1647 Testing shows that MKL provides higher performance for BLAS routines; especially on the Xeon Phi platform. A
1648 significant performance difference in favour of MKL has been also observed for matrix norm computations. On the
1649 other hand, PLASMA has proven superior to the other libraries for algorithms suited to tile-oriented implementation.
1650 This includes the LDL^T factorization, and QR factorization of tall and skinny matrices, where tiling readily provides
1651 potential for increased parallelism.
1652

1653 PLASMA offers an important advantage for operations composed of several base algorithms, such as solving a
1654 system of linear equations composed of matrix factorization and back-substitution. While executing the corresponding
1655 algorithms in a synchronous way suffers from lack of parallelism at the beginning and towards the end of the execution,
1656 asynchronous execution allows the merging of these parts of the execution. An operation with a potentially large
1657 performance advantage from such merging is computing an inverse of an SPD matrix. Thanks to the asynchronous
1658 execution, the performance of PLASMA is typically as much as two times higher than that of the other libraries.
1659

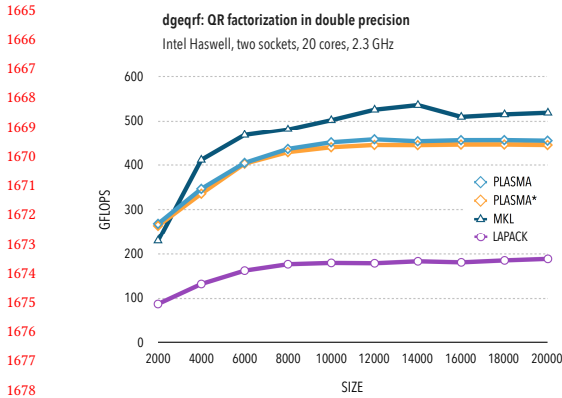


Fig. 52. Performance of dgeqrf on Haswell.

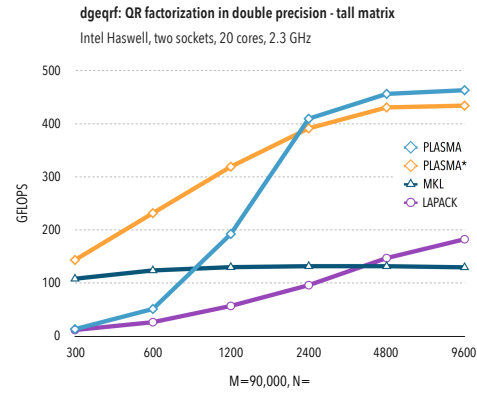


Fig. 53. Performance of dgeqrf on Haswell, tall matrix.

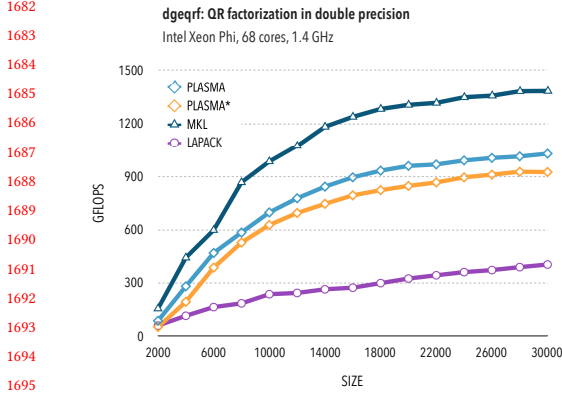


Fig. 54. Performance of dgeqrf on Phi.

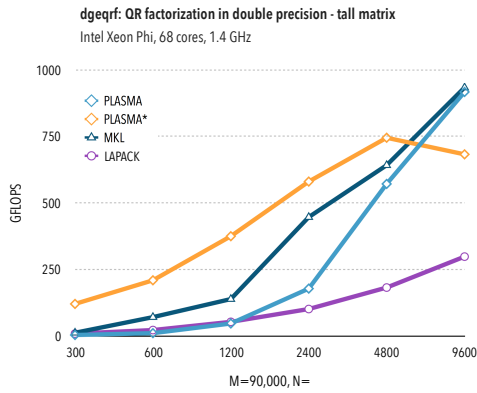


Fig. 55. Performance of dgeqrf on Phi, tall matrix.

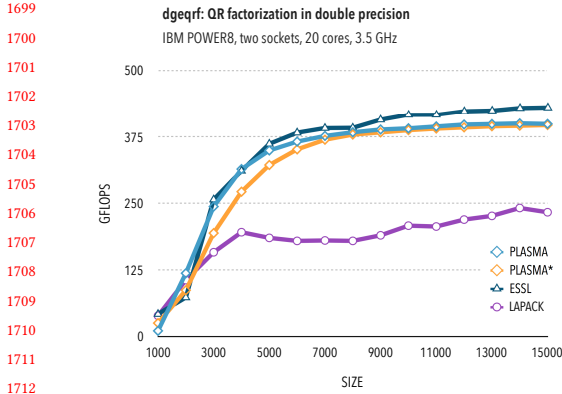


Fig. 56. Performance of dgeqrf on POWER8.

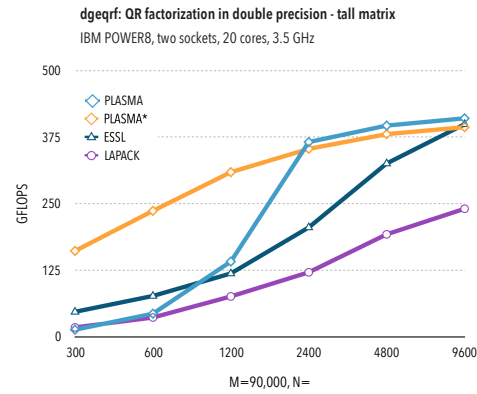


Fig. 57. Performance of dgeqrf on POWER8, tall matrix.

1717 PLASMA 17 currently does not contain all the functionality of the previous version. Specifically, extending the
 1718 library to eigenvalue problems and singular value decomposition is the current work in progress.
 1719

1720 REFERENCES

- 1721 Jan Ole Aasen. 1971. On the reduction of a symmetric matrix to tridiagonal form. *BIT Numerical Mathematics* 11, 3 (1971), 233–242. <https://doi.org/10.1007/BF01931804>
- 1722 Maksims Abalenkovs, Negin Bagherpour, Jack Dongarra, Mark Gates, Azzam Haidar, Jakub Kurzak, Piotr Luszczyk, Samuel Relton, Jakub Sistek, David
 1723 Stevens, Panruo Wu, Ichitaro Yamazaki, Asim YarKhan, and Mawussi Zounon. 2017b. *PLASMA 17 Performance Report*. Technical Report 292. LAPACK
 1724 Working Note. <http://www.netlib.org/lapack/lawnspdf/lawn292.pdf>
- 1725 Maksims Abalenkovs, Negin Bagherpour, Jack Dongarra, Mark Gates, Azzam Haidar, Jakub Kurzak, Piotr Luszczyk, Samuel Relton, Jakub Sistek, David
 1726 Stevens, Panruo Wu, Ichitaro Yamazaki, Asim YarKhan, and Mawussi Zounon. 2017a. *PLASMA 17.1 Functionality Report*. Technical Report 293.
 1727 LAPACK Working Note. <http://www.netlib.org/lapack/lawnspdf/lawn293.pdf>
- 1728 Ahmad Abdelfattah, Hartwig Anzt, Jack Dongarra, Mark Gates, Azzam Haidar, Jakub Kurzak, Piotr Luszczyk, Stanimire Tomov, Ichitaro Yamazaki, and
 1729 Asim YarKhan. 2016. Linear algebra software for large-scale accelerated multicore computing. *Acta Numerica* 25 (2016), 1–160.
- 1730 Emmanuel Agullo, Henricus Bouwmeester, Jack Dongarra, Jakub Kurzak, Julien Langou, and Lee Rosenberg. 2010. Towards an efficient tile matrix inversion
 1731 of symmetric positive definite matrices on multicore architectures. In *International Conference on High Performance Computing for Computational
 1732 Science*. Springer, 129–138. https://doi.org/10.1007/978-3-642-19328-6_14
- 1733 Emmanuel Agullo, Jim Demmel, Jack Dongarra, Bilel Hadri, Jakub Kurzak, Julien Langou, Hatem Ltaief, Piotr Luszczyk, and Stanimire Tomov. 2009.
 1734 Numerical linear algebra on emerging architectures: The PLASMA and MAGMA projects. In *Journal of Physics: Conference Series*, Vol. 180. IOP
 1735 Publishing, 012037.
- 1736 Edward Anderson, Zhaojun Bai, Christian Bischof, Susan L. Blackford, James W. Demmel, Jack J. Dongarra, Jeremy Du Croz, Anne Greenbaum, Sven J.
 1737 Hammarling, Alan McKenney, and Danny C. Sorensen. 1999. *LAPACK User's Guide* (Third ed.). Society for Industrial and Applied Mathematics,
 1738 Philadelphia.
- 1739 Marc Baboulin, Alfredo Buttari, Jack Dongarra, Jakub Kurzak, Julie Langou, Julien Langou, Piotr Luszczyk, and Stanimire Tomov. 2009. Accelerating
 1740 scientific computations with mixed precision algorithms. *Computer Physics Communications* 180, 12 (2009), 2526–2533. <https://doi.org/10.1016/j.cpc.2008.11.005>
- 1741 Grey Ballard, Dulcinea Becker, James Demmel, Jack Dongarra, Alex Druinsky, Inon Peled, Oded Schwartz, Sivan Toledo, and Ichitaro Yamazaki. 2014. A
 1742 Communication Avoiding Symmetric Indefinite Factorization. *SIAM J. Matrix Anal. Appl.* 35, 4 (2014), 1364–1406.
- 1743 Pieter Bellens, Josep M Perez, Rosa M Badia, and Jesus Labarta. 2006. CellSs: a programming model for the Cell BE architecture. In *SC 2006 Conference,
 1744 Proceedings of the ACM/IEEE*. IEEE, 5–5.
- 1745 Susan L. Blackford, Jaeyoung Choi, Andrew Cleary, Ed D'Azevedo, James W. Demmel, Inderjit Dhillon, Jack J. Dongarra, Sven J. Hammarling, Greg Henry,
 1746 Antoine Petitet, Ken Stanley, David W. Walker, and Clint R. Whaley. 1997. *ScaLAPACK User's Guide*. Society for Industrial and Applied Mathematics,
 1747 Philadelphia, PA, USA.
- 1748 George Bosilca, Aurelien Bouteiller, Anthony Danalis, Mathieu Faverge, Azzam Haidar, Thomas Herault, Jakub Kurzak, Julien Langou, Pierre Lemarinier,
 1749 Hatem Ltaief, Piotr Luszczyk, Asim YarKhan, and Jack Dongarra. 2011. Flexible Development of Dense Linear Algebra Algorithms on Massively
 1750 Parallel Architectures with DPLASMA. In *Proceedings of the 2011 IEEE International Symposium on Parallel and Distributed Processing Workshops
 1751 (IPDPSW '11)*. IEEE Computer Society, Washington, DC, USA, 1432–1441. <https://doi.org/10.1109/IPDPS.2011.299>
- 1752 George Bosilca, Aurelien Bouteiller, Anthony Danalis, Mathieu Faverge, Azzam Haidar, Thomas Herault, Jakub Kurzak, Julien Langou, Pierre Lemarinier,
 1753 Hatem Ltaief, Piotr Luszczyk, Asim Yarkhan, and Jack J. Dongarra. 2010a. *Distributed Dense Numerical Linear Algebra Algorithms on Massively Parallel
 1754 Architectures: DPLASMA*. Technical Report. Innovative Computing Laboratory, University of Tennessee. [http://icl.cs.utk.edu/news_pub/submissions/
 1755 ut-cs-10-660.pdf](http://icl.cs.utk.edu/news_pub/submissions/ut-cs-10-660.pdf)
- 1756 George Bosilca, Aurelien Bouteiller, Anthony Danalis, Mathieu Faverge, Azzam Haidar, Thomas Herault, Jakub Kurzak, Julien Langou, Pierre Lemarinier,
 1757 Hatem Ltaief, Piotr Luszczyk, Asim Yarkhan, and Jack J. Dongarra. 2010b. *Distributed-Memory Task Execution and Dependence Tracking within DAGuE
 1758 and the DPLASMA Project*. Technical Report 232. LAPACK Working Note. <http://www.netlib.org/lapack/lawnspdf/lawn232.pdf> UT-CS-10-660.
- 1759 George Bosilca, Aurelien Bouteiller, Anthony Danalis, Thomas Herault, Pierre Lemarinier, and Jack Dongarra. 2012. DAGuE: A generic distributed DAG
 1760 engine for High Performance Computing. *Parallel Comput.* 38, 1-2 (2012), 37–51.
- 1761 Henricus Bouwmeester and Julien Langou. 2010. A critical path approach to analyzing parallelism of algorithmic variants. Application to Cholesky
 1762 inversion. (2010). arXiv:1010.2000 <https://arxiv.org/abs/1010.2000>
- 1763 Alfredo Buttari, Jack Dongarra, Julie Langou, Julien Langou, Piotr Luszczyk, and Jakub Kurzak. 2007. Mixed precision iterative refinement techniques
 1764 for the solution of dense linear systems. *The International Journal of High Performance Computing Applications* 21, 4 (2007), 457–466. <https://doi.org/10.1177/1094342007084026>
- 1765 Alfredo Buttari, Julien Langou, Jakub Kurzak, and Jack Dongarra. 2008. Parallel tiled QR factorization for multicore architectures. *Concurrency and
 1766 Computation: Practice and Experience* 20, 13 (2008), 1573–1590. <https://doi.org/10.1002/cpe.1301>

1767 Manuscript submitted to ACM
 1768

- 1769 Alfredo Buttari, Julien Langou, Jakub Kurzak, and Jack Dongarra. 2009. A class of parallel tiled linear algebra algorithms for multicore architectures.
1770 *Parallel Comput.* 35, 1 (2009), 38–53. <https://doi.org/10.1016/j.parco.2008.10.002>
- 1771 Anthony Castaldo and Clint Whaley. 2010. Scaling LAPACK panel operations using parallel cache assignment. In *ACM Sigplan Notices*, Vol. 45. 223–232.
1772 <https://doi.org/10.1145/1693453.1693484>
- 1773 James W. Demmel, Laura Grigori, Mark F. Hoemmen, and Julien Langou. 2008. *Communication-optimal parallel and sequential QR and LU factorizations*.
1774 Technical Report 204. LAPACK Working Note. <http://www.netlib.org/lapack/lawnspdf/lawn204.pdf>
- 1775 Simplicé Donfack, Jack Dongarra, Mathieu Faverge, Mark Gates, Jakub Kurzak, Piotr Luszczek, and Ichitaro Yamazaki. 2015. A survey of recent
1776 developments in parallel implementations of Gaussian elimination. *Concurrency and Computation: Practice and Experience* 27, 5 (2015), 1292–1309.
1777 <https://doi.org/10.1002/cpe.3306>
- 1778 Jack Dongarra, Mathieu Faverge, Thomas Héroult, Mathias Jacquelin, Julien Langou, and Yves Robert. 2013. Hierarchical QR factorization algorithms for
1779 multi-core clusters. *Parallel Comput.* 39, 4–5 (2013), 212–232. <https://doi.org/10.1016/j.parco.2013.01.003>
- 1780 Jack Dongarra, Mathieu Faverge, Hatem Ltaief, and Piotr Luszczek. 2014. Achieving numerical accuracy and high performance using recursive tile LU
1781 factorization with partial pivoting. *Concurrency and Computation: Practice and Experience* 26, 7 (2014), 1408–1431. <https://doi.org/10.1002/cpe.3110>
- 1782 Jack J. Dongarra, J. Du Croz, Iain S. Duff, and Sven J. Hammarling. 1990a. Algorithm 679: A Set of Level 3 Basic Linear Algebra Subprograms. *ACM Trans.*
1783 *Math. Software* 16 (1990), 1–17.
- 1784 Jack J. Dongarra, J. Du Croz, Iain S. Duff, and Sven J. Hammarling. 1990b. A Set of Level 3 Basic Linear Algebra Subprograms. *ACM Trans. Math. Software*
1785 16 (1990), 18–28.
- 1786 Jack J. Dongarra, J. Du Croz, Sven J. Hammarling, and R. Hanson. 1988a. Algorithm 656: An Extended Set of FORTRAN Basic Linear Algebra Subprograms.
1787 *ACM Trans. Math. Software* 14 (1988), 18–32.
- 1788 Jack J. Dongarra, J. Du Croz, Sven J. Hammarling, and R. Hanson. 1988b. An Extended Set of FORTRAN Basic Linear Algebra Subprograms. *ACM Trans.*
1789 *Math. Software* 14 (1988), 1–17.
- 1790 Mathieu Faverge, Julien Langou, Yves Robert, and Jack Dongarra. 2016. Bidiagonalization with Parallel Tiled Algorithms. (2016). arXiv:1611.06892
1791 <https://arxiv.org/abs/1611.06892>
- 1792 Fred Gustavson, Lars Karlsson, and Bo Kågström. 2012. Parallel and cache-efficient in-place matrix storage format conversion. *ACM Trans. Math. Software*
1793 38, 3 (2012), 17.
- 1794 Azzam Haidar, Heike Jagode, Asim YarKhan, Phil Vaccaro, Stanimire Tomov, and Jack Dongarra. 2017. Power-aware computing: Measurement, control,
1795 and performance analysis for Intel Xeon Phi. In *2017 IEEE High Performance Extreme Computing Conference (HPEC)*. 1–7. <https://doi.org/10.1109/HPEC.2017.8091085>
- 1796 Azzam Haidar, Hatem Ltaief, Asim YarKhan, and Jack Dongarra. 2011. Analysis of Dynamically Scheduled Tile Algorithms for Dense Linear Algebra on
1797 Multicore Architectures. *Concurr. Comput. : Pract. Exper.* 24, 3 (2011), 305–321. <https://doi.org/10.1002/cpe.1829>
- 1798 Nicholas J. Higham. 2002. *Accuracy and Stability of Numerical Algorithms* (2nd ed.). Society for Industrial and Applied Mathematics (SIAM), Philadelphia.
- 1799 Bo Kågström, Per Ling, and Charles van Loan. 1998. GEMM-based Level 3 BLAS: High-performance Model Implementations and Performance Evaluation
1800 Benchmark. *ACM Trans. Math. Software* 24, 3 (1998), 268–302. <https://doi.org/10.1145/292395.292412>
- 1801 Jakub Kurzak, Alfredo Buttari, and Jack Dongarra. 2008. Solving systems of linear equations on the CELL processor using Cholesky factorization. *IEEE*
1802 *Transactions on Parallel and Distributed Systems* 19, 9 (2008), 1175–1186.
- 1803 Jakub Kurzak and Jack Dongarra. 2006. Implementing linear algebra routines on multi-core processors with pipelining and a look ahead. In *International*
1804 *Workshop on Applied Parallel Computing*. Springer, 147–156.
- 1805 Jakub Kurzak and Jack Dongarra. 2007. Implementation of mixed precision in solving systems of linear equations on the CELL processor. *Concurrency*
1806 *and Computation: Practice and Experience* 19, 10 (2007), 1371–1385.
- 1807 Jakub Kurzak and Jack Dongarra. 2009. QR factorization for the Cell Broadband Engine. *Scientific Programming* 17, 1-2 (2009), 31–42.
- 1808 Jakub Kurzak, Piotr Luszczek, Asim YarKhan, Mathieu Faverge, Julien Langou, Henricus Bouwmeester, and Jack Dongarra. 2013. Multithreading in the
1809 PLASMA Library. *Multicore Computing: Algorithms, Architectures, and Applications* (2013), 119.
- 1810 Julie Langou, Julien Langou, Piotr Luszczek, Jakub Kurzak, Alfredo Buttari, and Jack Dongarra. 2006. Exploiting the performance of 32 bit floating point
1811 arithmetic in obtaining 64 bit accuracy (revisiting iterative refinement for linear systems). In *SC 2006 Conference, Proceedings of the ACM/IEEE*. IEEE,
1812 50–50. <https://doi.org/10.1109/SC.2006.30>
- 1813 Charles L. Lawson, Richard J. Hanson, David Kincaid, and Fred T. Krogh. 1979. Basic Linear Algebra Subprograms for FORTRAN usage. *ACM Trans.*
1814 *Math. Software* 5 (1979), 308–323.
- 1815 Miroslav Rozložník, Gil Shklarski, and Sivan Toledo. 2011. Partitioned triangular tridiagonalization. *ACM Trans. Math. Software* 37, 4 (2011), 1–16.
- 1816 Herb Sutter. 2005. The free lunch is over: A fundamental turn toward concurrency in software. *Dr. Dobbs's Journal* 30, 3 (2005), 202–210.
- 1817 Ichitaro Yamazaki, Jakub Kurzak, Panrui Wu, Mawussi Zounon, and Jack Dongarra. 2018. Symmetric Indefinite Linear Solver using OpenMP Task on
1818 Multicore Architecture. *IEEE Transactions on Parallel & Distributed Systems* (2018). <https://doi.org/10.1109/TPDS.2018.2808964> To appear.
- 1819 Asim YarKhan, Jakub Kurzak, Piotr Luszczek, and Jack Dongarra. 2016. Porting the PLASMA numerical library to the OpenMP standard. *International*
1820 *Journal of Parallel Programming* 45, 3 (2016), 1–22. <https://doi.org/10.1007/s10766-016-0441-6>